

PCCP

Accepted Manuscript



This article can be cited before page numbers have been issued, to do this please use: J. Yong, J. Huo, F. Chen, Q. Yang and X. Hou, *Phys. Chem. Chem. Phys.*, 2018, DOI: 10.1039/C8CP04009E.



This is an Accepted Manuscript, which has been through the Royal Society of Chemistry peer review process and has been accepted for publication.

Accepted Manuscripts are published online shortly after acceptance, before technical editing, formatting and proof reading. Using this free service, authors can make their results available to the community, in citable form, before we publish the edited article. We will replace this Accepted Manuscript with the edited and formatted Advance Article as soon as it is available.

You can find more information about Accepted Manuscripts in the author guidelines.

Please note that technical editing may introduce minor changes to the text and/or graphics, which may alter content. The journal's standard <u>Terms & Conditions</u> and the ethical guidelines, outlined in our <u>author and reviewer resource centre</u>, still apply. In no event shall the Royal Society of Chemistry be held responsible for any errors or omissions in this Accepted Manuscript or any consequences arising from the use of any information it contains.



View Article Online

Oil/Water Separation Based on the Natural Materials with 10.1039/C8CP04009E **Super-Wettability: Recent Advances**

Jiale Yong^{1,3}, Jinglan Huo^{1,3}, Feng Chen^{1,3,*}, Qing Yang^{2,3}, and Xun Hou¹

¹State Key Laboratory for Manufacturing System Engineering and Shaanxi Key Laboratory of Photonics

Technology for Information, School of Electronics & Information Engineering, Xi'an Jiaotong University,

Xi'an, 710049, PR China

²School of Mechanical Engineering, Xi'an Jiaotong University, Xi'an, 710049, PR China

³The International Joint Research Laboratory for Micro/Nano Manufacturing and Measurement Technologies,

Xi'an Jiaotong University, Xi'an, 710049, PR China

*Corresponding author: chenfeng@mail.xjtu.edu.cn

Abstract

The frequency of oil spills and the increasing amount of oily sewages not only cause serious water pollution as well as a lot of ecological problems but also result in huge economic losses. To address such problems, developing advanced technologies and materials for achieving efficient oil/water separation is a critical way and emerging as a hot research topic nowadays. Herein, we have reviewed the recent developments in oil/water separation by using superwetting porous materials, mainly focusing on the natural materials. By using the natural materials as the examples, we show how to use the superwetting porous materials to separate different mixtures of water and oil, including the inherent superwettability of the natural materials, separating method/process, and separation mechanism. The natural superwetting materials are usually low-cost, eco-friendly, and can be easily obtained, so the oil/water separation based on the natural materials is the great promise to address above-mentioned globally recognized oil contamination challenge. In addition, these natural examples seem more attractive to the general researcher who is new to this field as well as the expert and even common people, since natural materials look more interesting than artificial complex materials. We believe our review will help beginners better understand the significance, application value, mechanism and principle of oil/water separation by superwetting porous materials.

Keywords: oil/water separation, superwettability, natural materials. superhydrophobicity, underwater superoleophobicity

View Article Online DOI: 10.1039/C8CP04009E

1. Introduction

Published on 17 September 2018. Downloaded by Gazi Universitesi on 9/17/2018 5:30:59 AM

The progress of human society allows our life to become better, but many environmental and energy issues also appear associated with such progress. As the global demand for energy continues to grow, oil-spill accidents and industrial oily wastewater discharges occur frequently.¹⁻⁸ For example, in 1989, the Exxon Valdez oil tanker ran aground on Bligh Reef and spilled 11 million gallons of oil into Alaska's Prince William Sound. In 2002, the tanker Prestige encountered a storm and split up at sea, spreading 20 million gallons of heavy fuel oil onto Spanish coasts.⁷ In 2010, the Gulf of Mexico oil spill resulted in 200 million gallons of crude oil being released into the sea (Figure 1a,b).8 In the remarks (June of that year) from Oval Office, U.S. President Barack Obama called the Gulf of Mexico oil spill "the worst environmental disaster America has ever faced.". 9 Most animals and plants living in the waters near the incident area died (Figure 1c,d). On the other hand, much oily wastewater is largely produced from many industries every day, such as mining, metal smelting, textiles, biopharmaceuticals, petrochemicals, and foods. Such oily sewage has already become one kind of the common pollutants around the world and is now a serious global environmental concern. The frequency of oil spills and the oily sewages not only cause severe water pollution as well as a lot of ecological problems but also result in huge economic losses. 6-12 To address the above-mentioned problems, researchers have developed various technologies and materials for achieving effective oil/water separation until now, and oil/water separation is still a hot research topic to protect the environment and reduce economic loss nowadays. 1-5 Indeed, an explosive growth of published papers describing oil/water separation has occurred in recent years, as shown in Figure 2.



Figure 1. Gulf of Mexico oil spill accident. (a,b) Leaked crude oil covering on the ocean surface. (c,d) Seabirds and sea turtles being killed by the leaked crude oil. Reproduced from ref. 5 with permission from the Editorial office of Acta Physico-Chimica Sinica, copyright 2018.

View Article Online DOI: 10.1039/C8CP04009E

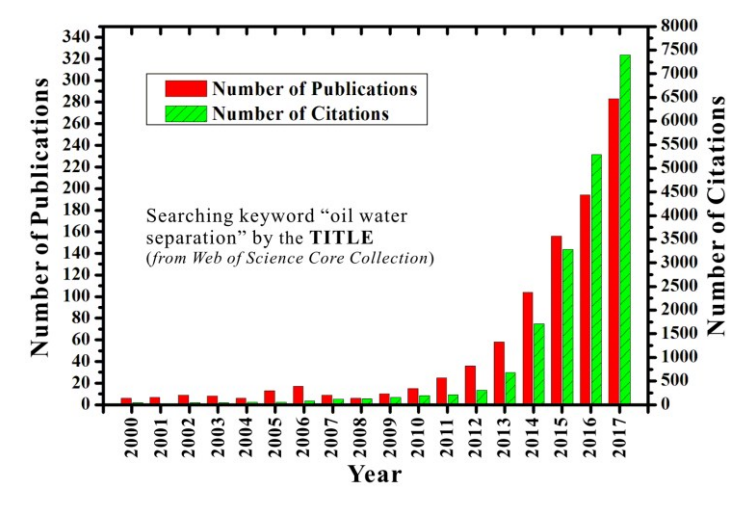


Figure 2. Numbers and corresponding citations of the published articles related to oil/water separation indexed in ISI Web of Science by the title of "oil water separation".

Conventional methods for oil/water separation include absorption, gravity separation, skimming, flotation, centrifugation, and so on. 1,4 Although above methods could also make certain effects in handling most oil/water mixtures, these methods usually suffer from many limitations such as low separation efficiency, the need of an external input of driving energy, and the generation of secondary pollutants. For example, porous materials such as sponges, foams, and textiles are commonly used to absorb oils from water once in emergency situations such as oil-leakage/spillage accidents occur. However, such materials simultaneously absorb oil and water, resulting in poor separation selectivity and low efficiency. The reuse of the separated oils is very difficult because the purity cannot meet the minimum requirement for reuse. Moreover, these materials do not have anti-oil-contamination ability. They lose absorbing function after just once separation, and then are generally burned or buried in the ground. Such treatment causes secondary environmental pollution with the release of toxic gases and land contamination. Above limitations drive people to further develop more effective separating materials and systems.

Recently, superwetting micro-porous materials (i.e., their surfaces show superhydrophobicity-superoleophilicity or superoleophobicity-superhydrophilicity) have been successfully introduced into the research field of oil/water separation because water and oil have different interface effects, and such materials show great separating performance compared to the conventional materials. The superwettability can be obtained by designing appropriate surface microstructures and chemical composition on material surfaces. In 2004, Feng et al. fabricated an in-air superhydrophobic and superoleophilic polytetrafluoroethylene (PTFE) coated metal mesh. This mesh could separate the mixture of water and oil because the mesh only allowed oil to penetrate through. This kind of superhydrophobic porous materials is usually called "oil removing" material. In order to avoid the problem that "oil removing" materials are easily contaminated and blocked by oil adhesion, in 2011, Xue et al. put forward a new strategy of using underwater superoleophobic porous membrane (i.e., hydrogel-coated stainless steel mesh) to separate the oil/water

mixtures. 21 The as-prepared mesh exhibited superhydrophilicity in air and became / C8CP04009E superoleophobic after the immersion in water. Therefore, the pre-water-wetted mesh only allowed water to penetrate through, showing "water removing" property. Following the above-mentioned achievements, an increasing number of porous materials with various superwettabilities were developed and successfully applied in oil/water separation (Figure 2). 1-4,13-35 Although those superwetting materials have a satisfactory separating ability, some existing disadvantages still restrict those materials to just the laboratory and hinder the large-scale practical applications of them. 11,45 The cost of the materials, the expensive equipment required, the complex preparation process, and the human labor for constructuring superwetting microstructures will become tremendous burden towards the large-scale application. Another issue is secondary pollution. The surfaces of the most widely used materials have rough superwetting microstructures, which are generally formed by chemical corrosion, surface modification, or other chemical treatments. 1,2 The waste produced to create the separating materials will cause a new environmental problem (disposing of the waste). Therefore, taking into account the large-scale practical application, a simple, low-cost, eco-friendly, green route that can efficiently separate large amounts of the mixtures of water and oil is highly desired.

In this article, we will review the recent developments in oil/water separation by using porous superwetting materials, mainly focusing on the natural materials. The article starts with a brief introduction of the urgency and significance of developing oil/water separating technology. Then, three typical separating ways based on the superhydrophobicity or superoleophobicity of porous materials are presented. The next part shows several natural materials, one by one, with various inherent superwettabilities that are successfully applied in oil/water separation, including the wettability, separating method/process, and the separation mechanism of each case. Natural materials look more interesting than artificial complex materials. Thereby, these natural examples seem more attractive to advanced undergraduates, the general research chemists as well as the experts. Finally, a brief discussion of current challenges and prospects in this area is provided in our own perspective. We believe our review will help beginners better understanding the significance, application value, mechanism and principle of oil/water separation by superwetting porous materials.

2. Mechanism of oil/water separation by superwetting porous

materials

Published on 17 September 2018. Downloaded by Gazi Universitesi on 9/17/2018 5:30:59 AM

2.1 Superhydrophobic mesh/membranes

In 2004, Jiang et al. first reported an artificial superhydrophobic and superoleophilic metal mesh that could be used for the effective separation of oil and water. ¹³ A micro/nanoscale hierarchical structure was generated on the surface of a stainless steel mesh by spraying the homogeneous emulsion containing PTFE with low surface energy onto the mesh surface. Figure 3a-c shows the scanning electronic microscopy

(SEM) images of the surface microstructure of the resultant rough mesh. After the /cacpo4009E coating treatment, the meshes still kept open without blocking (Figure 3a). Due to the synergy effect of the resultant hierarchical microstructure and the intrinsic chemical property of PTFE substrate (i.e., inherent hydrophobicity and oleophilicity), the PTFE coated mesh was endowed with both superhydrophobicity and superoleophilicity in air. Water droplet on such mesh could maintain a ball shape with contact angle (CA) of 156.2 ± 2.8 °(Figure 3d), and could easily roll off as long as the mesh was tilted 4 °. Such ultralow adhesive superhydrophobicity is ascribed to that water droplet on the structured mesh surface is at the Cassie wetting state (Figure 3f). An air layer is trapped in the rough microstructure and forms an air cushion underneath the droplet, which prevents the water droplet from effectively touching the surface of the PTFE coated mesh. In contrast, when a diesel oil droplet was dropped onto the mesh, it would rapidly spread out and finally permeate through the mesh within 240 ms (Figure 3e). The inverse superwettability of the as-prepared mesh to water (superhydrophobicity) and oil (superoleophilicity), respectively, makes the mesh be effectively applied in the separation of diesel oil and water. As shown in Figure 3g, when the oil/water mixture is poured onto the mesh film, water phase in the mixture is repelled by the mesh because of superhydrophobicity thereby always stay above the mesh, whereas the superoleophilicity results in that oil wets the rough mesh and further passes through the mesh, achieving separation.

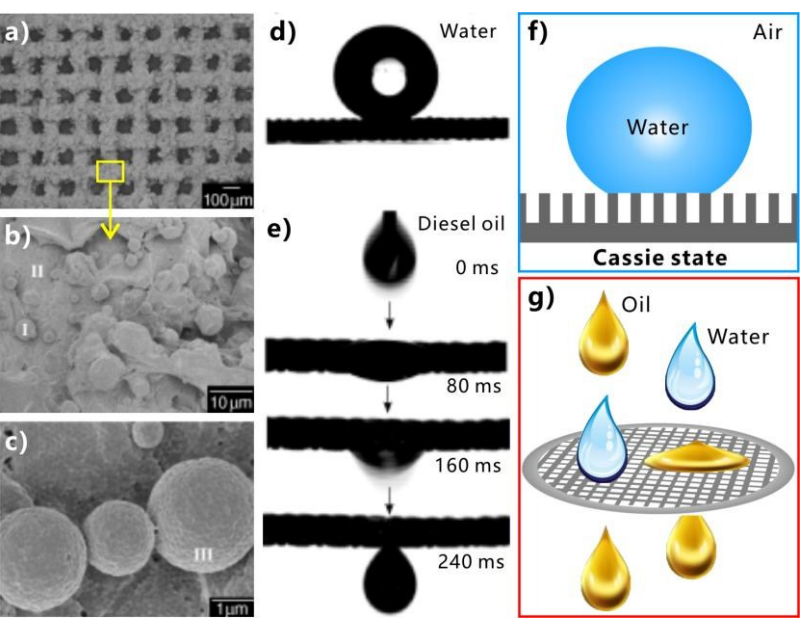


Figure 3. Achievement of oil/water separation based on the superhydrophobic and superoleophilic mesh. (a-c) SEM images of the PTFE-coated stainless steel mesh. (d) Shape of a water droplet on the as-prepared mesh. (e) Process of a diesel oil droplet permeating through the as-prepared mesh. (f) Schematic diagram showing the Cassie wetting state. (g) Schematic diagram showing the separation mechanism by using a superhydrophobic and superoleophilic mesh. Reproduced from ref. 13 with permission from Wiley, copyright 2004.

Following the above separating principle, various superhydrophobic meshes and membranes have been developed for achieving efficient oil/water separation. ^{16-18,46-62} For example, Wang et al. deposited a rough copper layer onto a copper mesh substrate

by electrochemical deposition.¹⁴ Copper sulfate solution was used as the electrolytegy/C8CP04009E After further modification of the structured mesh with long-chain fatty acid, the resultant copper mesh showed superhydrophobicity and superoleophilicity in air. The mixture of diesel and water was successfully separated by the mesh. Kong et al. simply immersed a commercial phosphor-copper mesh in distilled water at room temperature for 3 h to deposit highly dense ordered Cu₂O nanorods on the mesh.¹⁵ After the 1-dodecanethiol surface modification, the mesh with Cu₂O nanostructures became superhydrophobic and superoleophilic. The as-prepared mesh could separate the diesel-water and the hexane-water mixtures. Song et al. prepared a micro/nanoscale hierarchical rough stainless steel mesh with superhydrophobicity by a chemical etching method. 16 The stainless steel mesh was firstly immersed in the solution composed of 1 mol·L⁻¹ CuCl₂ and 1 mol·L⁻¹ HCl to generate surface microstructures. Then, the mesh was treated with stearic acid to lower surface free energy. Based on the superhydrophobic mesh, an oil/water separating device was designed. Li et al. used the flame of paraffin candle to burn the surface of a stainless steel mesh to coat the metal mesh surface with a layer of nanoscale particles. 17 The color of the coated mesh turned to black because of the deposition of candle soot layer. Subsequently, the smaller hydrophobic silica nanoparticles were deposited on the candle soot-coated mesh. The as-prepared mesh had both superhydrophobicity and superoleophilicity, and could even repel hot water and strong corrosive liquids. The superhydrophobic mesh was able to separate various oils and organic solvents like kerosene, toluene, petroleum ether, heptanes, and chloroform from water with separation efficiency above 99.0%. Moreover, the mesh also presented excellent environmental stability for separating the mixtures of oil and hot water and different corrosive solutions. Huang et al. applied a one-pot hydrothermal reaction to obtain large-scale flower-like TiO₂ particles-coated cotton fabrics. ¹⁸ The surface wettability superhydrophilicity TiO₂@fabrics changed from superhydrophobicity and superoleophilicity by a hydrogen-bond-driven process via fluoroalkylsilane modification. The superhydrophobic fabrics exhibited remarkable mechanical and environmental stability and could selectively separate oil from various water/oil mixtures. Moreover, the separating process was easy to recycle. Xue et al. fabricated superhydrophobic and superoleophilic textiles by a continuous "double-dip double-nip" method. 19 The commercially available poly(ethylene terephthalate) (PET) textiles were firstly dipped into ethanol and nipped by two rolls under the pressure of 20 Mpa. Then, the textiles were dipped into a polydimethylsiloxane (PDMS)-based solution and nipped again under the pressure of 0.2 Mpa. The dried textiles showed great superhydrophobicity/superoleophilicity and had the ability to separate the mixture of water and hexane. Yong et al. created a kind of rough microstructure on the thin PTFE sheet by femtosecond laser ablation.²⁰ The ablated surface exhibited durable ultralow-adhesive superhydrophobicity even after storing in various harsh environments (e.g., strong acid, strong alkali, and high temperature) for a long time. A through microholes array was further generated on the rough superhydrophobic sheet by a subsequent mechanical drilling process. When oil and water droplets were dropped onto the sheet, oil droplets would spread out quickly

and penetrate through the microholes array-structured superhydrophobic PTFE sheet / C8CP04009E whereas water droplets were prevented and maintained on the sample surface. Taking advantages of the inverse superhydrophobicity and superoleophilicity, the as-prepared sheet was successfully applied in the field of oil/water separation and is also very efficient to separate the mixtures of oil and corrosive acid/alkali solutions, exhibiting strong potential for practical application. Cortese et al. fabricated superhydrophobic and superoleophilic diamond-like carbon-coated cotton textiles through plasma-enhanced chemical vapor deposition.⁴⁹ The resultant cotton textiles could separate water from a broad variety of oils and organic solvents (e.g., vegetable oil, diesel, gasoline, and crude oil) using gravity. Crick et al. coated various copper meshes with extremely rough silicone elastomer films.⁵⁹ The coating of the polymer was carried out by aerosol assisted chemical vapor deposition and endowed the mesh with superhydrophobicity. Organic solvents (hexane, petroleum ether and toluene) could be easily removed from water by using the superhydrophobic polymer-coated copper mesh. Singh et al. obtained zirconia-coated cotton fabrics with superhydrophobicity, superoleophilicity, and photocatalytic property.⁶⁰ The fabric could separate the mixtures of water and a series of oils with the efficiency above 99% even after repeated use for 10 cycles. Even though the coated fabric was suffered from harsh conditions (acidic, alkaline, salty, ultraviolet irradiation, and mechanical abrasion), its superhydrophobic/oleophilicity was still retained. Such durability allowed the fabric to work for a long period in the oil/water separation.

2.2 Underwater superoleophobic mesh/membranes

In 2011, Jiang et al. further fabricated a novel superhydrophilic and underwater superoleophobic metal mesh by coating the environment-friendly polyacrylamide hydrogel onto a stainless steel mesh.²¹ The hydrogel modification not only endowed the mesh surface with hydrophilic chemical composition but also resulted in a large number of nanoscale papillae structures on the resultant mesh surface (Figure 4a,b), which made the mesh be superhydrophilic in air and underwater superoleophobic (in an oil/water/solid three-phase system). In a water medium, the CA of an oil droplet on the rough mesh reached up to 155.3 \pm 1.8 ° (Figure 4c). The mesh also showed a very low adhesion to the underwater oil droplet (Figure 4d). As shown in Figure 4g, when the superhydrophilic rough substrate (such as the hydrogel coated stainless steel mesh) is immersed in water, water will fully wet the substrate and be filled in the space of the rough microstructure, forming a trapped water layer. Water is an ideal oil-repellent material, so the trapped water layer can provide the oil-repulsive force to prevent the effective contact between the underwater oil droplet and the textured mesh. Such oil wettability can be considered as an underwater version of Cassie wetting state (Figure 4g). When the mixture of water and crude oil was poured onto the as-prepared mesh film that was previously wetted by water, water in the mixture could permeate through the mesh while the oil was intercepted above the mesh (Figure 4e,f). As a result, the oil/water mixture was successfully separated. Such separating process could apply to a series of mixtures of water and various oils, with high separation efficiency (>99%). Figure 4h depicts the mechanism of separating an oil/water

mixture by using a pre-wetted underwater superoleophobic mesh. Oil phase in the /cacpo4009E mixture is repelled by the pre-wetted mesh and unable to pass through the mesh because of the superoleophobicity (in water) of the textured mesh, but water can wet the rough superhydrophilic mesh and then permeate through the mesh.

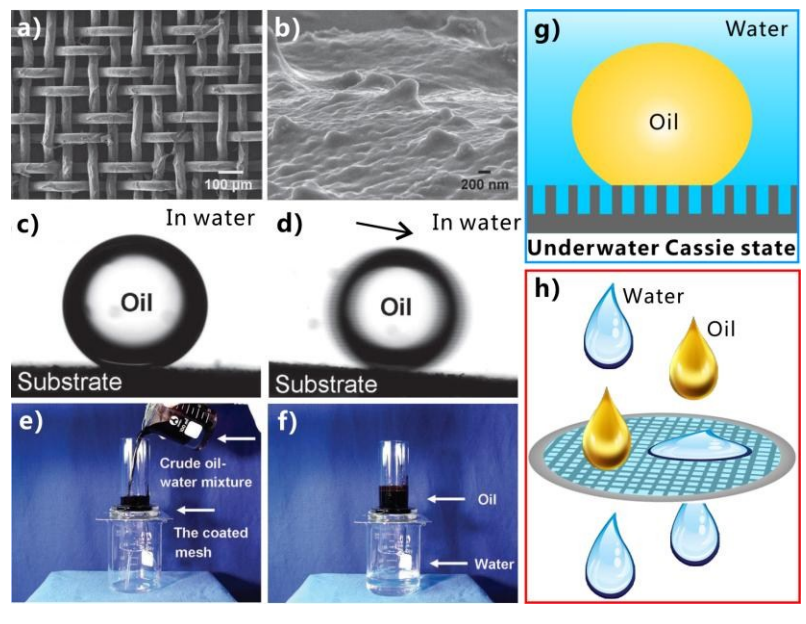


Figure 4. Achievement of oil/water separation based on the pre-wetted underwater superoleophobic mesh. (a,b) SEM images of the hydrogel-coated stainless steel mesh. (c) Static shape and (d) rolling behavior of an oil droplet on the as-prepared mesh in a water medium. (e,f) Separating the mixture of water and crude oil by using the pre-wetted as-prepared mesh: (e) before separation, (f) after separation. (g) Schematic diagram showing the underwater Cassie wetting state. (h) Schematic diagram showing the separation mechanism by using a water-wetted underwater superoleophobic mesh. Reproduced from ref. 21 with permission from Wiley, copyright 2011.

Published on 17 September 2018. Downloaded by Gazi Universitesi on 9/17/2018 5:30:59 AM.

Inspired by Jiang's work, a large number of underwater superoleophobic porous materials have been applied in the field of oil/water separation. 63-80 Wen et al. coated a stainless steel mesh with zeolite to endow the mesh surface with fine nanoscale rough structures apart from its inherent microscale meshes.²² The zeolite-coated mesh had excellent underwater superoleophobicity and was able to separate different oil/water mixtures in a harsh environment. Similarly, Liu et al. deposited graphene oxide layer on a stainless steel mesh and opened the meshes by subsequent oxygen plasma irradiation from the mesh's back.²³ When the mesh was immersed in water and an oil droplet was placed onto the resultant surface, the oil droplet kept a sphere, revealing excellent underwater superoleophobicity of the graphene oxide-coated mesh. The mixture of water and bean oil, which simulated the kitchen sewage, could be efficiently separated by such pre-wetted mesh. Zhang et al. fabricated a superhydrophilic and underwater superoleophobic Cu(OH)2 nanowires-structured copper mesh by a chemical-based oxidation method.²⁴ The copper mesh was just treated by immersing in the aqueous solution of NaOH and (NH₄)₂S₂O₈. The resultant mesh showed excellent separating capacity for not only water-rich immiscible mixtures but also dispersed oil/water mixtures. In addition, the mesh could withstand

the corrosion of strong acid and alkali, and had strong anti-pollution ability. Zhang View Article Online al. deposited the Cu ions from the electrolyte on the surface of a copper mesh substrate via a simple electrodeposition process. 25 The as-prepared rough porous mesh showed high superoleophobicity and ultralow adhesion to an underwater 1,2-dichloroethane droplet, with the oil CA (OCA) of 162° and oil sliding angle (OSA) less than 2°. The mesh has a good environmental stability for separating acid and alkali mixtures of water and oil, with the separating efficiency higher than 99%. By using a heat treatment, Yu et al. prepared rough nanoscale texture on the surface of nickel mesh substrate.²⁶ Combined with inherent micro-meshes, the as-prepared meshes with the micro/nanoscale hierarchical structure superhydrophilicity in air and superoleophobicity underwater. The mesh could separate different oil/water mixtures in harsh environments with high efficiency, reusability, and durability. Tao et al. used the non-woven fabric as the support to fabricate a hierarchical rough poly(vinylidene fluoride) (PVDF) membrane via phase inversion method and subsequent peeling process.²⁷ There were lots of pores with the diameter of 50-100 µm randomly distributing on the membrane surface. The surrounding area of the micro-pores was covered by the tightly packed spherulites of several micrometers and the nano-fibrils. The multi-scale rough microstructures resulted in both underwater superoleophobicity and underoil superhydrophobicity of the as-prepared membrane surface. The membrane was able to separate different kinds of oil/water emulsions, involving both oil-in-water and water-in-oil emulsions. Gao et al. reported an underwater superoleophobic nitrocellulose membrane with both microscale and nanoscale pores.²⁸ The nanopores were intrinsic structure of the nitrocellulose membrane, and the perforated microscale holes array was fabricated by a facile perforating method. A variety of oil/water mixtures (including gasoline, diesel, hexane, petroleum ether, high-viscosity crude oil/water mixtures, and even corrosive oil/water mixture) were successfully separated by the resultant membrane with a high separation efficiency (>99%). The penetration of water was very slow for the original membrane only with overlapped nanopores, while the microscale pores made water penetrate faster and easier through the dual-porous membrane. Li et al. fabricated a series of micropores-array-structured ultrathin aluminum foils by femtosecond laser perforating.²⁹ Every laser ablated point finally formed a single micropore with the diameter ranging from 2.4 to 32 µm. By using the typical point-by-point ablation process, a uniform through micropores array was created on the aluminum foil. The as-prepared foils were superhydrophilic in air with water CA (WCA) of 7.8° and switched to superoleophobic after the immersion in water. The measured OCAs were 153.1 ° to an underwater 1,2-dichloroethane droplet and 153.5 ° to an octane droplet, respectively. The opposite wettabilities for water and oil allowed the porous aluminum foil to have great oil/water separating function. Gondal et al. endowed stainless steel meshes with underwater superoleophobicity by spray deposition of nanostructured TiO₂ on the substrates.⁷⁶ Oil/water separation with the efficiency of 99% could be achieved through the coated mesh. Such fabrication method can be used to develop a large-scale oil/water separating device via coating large surface areas. Joo et al. proposed a simple synthetic route to generate cross-linked ionic polymers in

the vapor phase. 77 After the surface modification of a stainless steel mesh with the View Article Online polymer thin film, the resultant mesh showed hydrophilicity/underwater oleophobicity and could be successfully applied in oil/water separation. Chaudhary et al. obtained superhydrophilic porous foam membrane by blending gelatin, agarose and natural cross-linker.⁷⁸ Such porous membrane had some advantageous features in the application of oil/water separation. For example, the biodegradability makes it an eco-friendly material in comparison to the conventional separating mediums.

2.3 Oil-absorption 3D porous materials

Different from the superhydrophobic or underwater superoleophobic separating mesh/membranes, three-dimensional (3D) porous bulk materials can also be used to separate the oil/water mixture based on an absorption manner.⁸¹⁻¹⁰¹ Oil absorbent material is one of the most promising materials to clean oil from contaminated areas. Traditional absorbents are mainly 3D materials and are rich in pores, such as porous inorganic minerals (activated carbon, zeolites, clay, silica aerogels, and exfoliated graphite) and organic synthetic porous polymers (polyurethane (PU) foams, nonwoven polypropylene, and rubbers). However, those materials usually have ordinary surface wettability, so they also absorb water in addition to the leaked oils. As a result, the collected oils cannot be reused because they still contain water impurities, and the absorption process cannot be repeated. To improve the oil-absorption capacity and reusability, superhydrophobic and superoleophilic 3D porous materials have been developed recently, and such oil absorbent materials have attracted more and more attention. 30-35 As shown in Figure 5a, when this kind of porous materials is in contact with the mixture of water and oil, the water phase in the mixture is repelled by the materials and unable to enter into the inner porous space of the 3D materials because of superhydrophobicity of the material surfaces, while oils can be quickly absorbed by the materials driven by superoleophilicity and capillary action.³⁰ With shifting the materials to another place, the oil is removed from the mixture and can be released just by squeezing. The separation process can be continuously repeated by the cycle of oil absorption, transferring, and squeezing. The oils no matter on water surface or underwater can be completely removed from the oil/water mixture and be collected for reuse. Achieving oil/water separation by using oil-absorption 3D materials is better than using separating membrane in some special cases. For example, if a small amount of oil is leaked to the sea surface, we can just remove the oil by an oil-absorption material. In contrast, we need to pour a large volume of the mixture of the oil and seawater into the separating device based on 2D porous filtering membrane, costing a lot of manpower and resources. For the case of leaked heavy oils, the filtering method by using superwetting porous membrane might not be possible because the oils are underwater and transferring the oil/water mixture is very difficult, but the oil-absorption materials are able to directly take the underwater oils out of the water.

View Article Online DOI: 10.1039/C8CP04009E

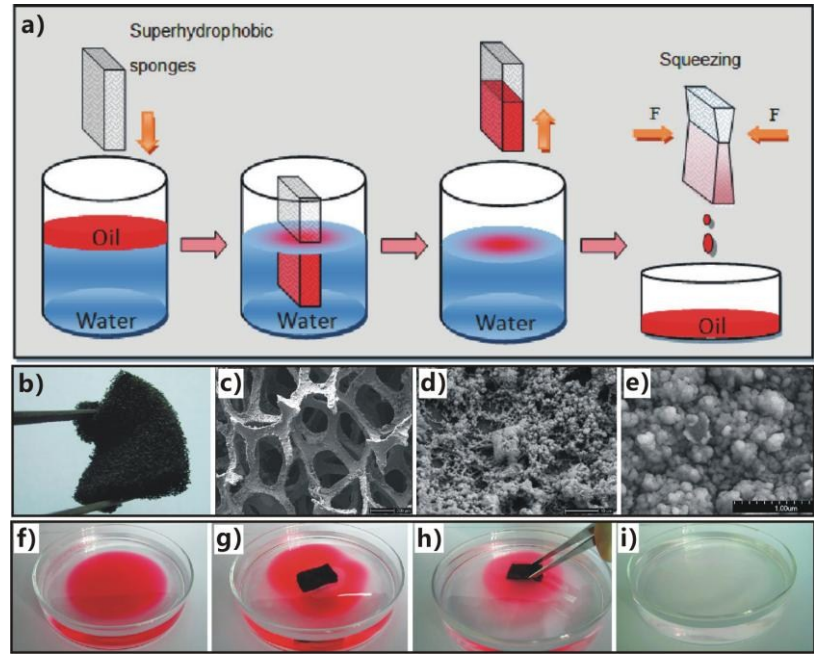


Figure 5. Removing and collecting oils from water surface by using a superhydrophobic and superoleophilic sponge. (a) Illustration for the oil/water separating mechanism and process. (b) Photography of a superhydrophobic sponge fabricated by solution-immersion processes. (c-e) SEM images of the framework surface of the as-prepared sponge. (f-h) Selective absorption of oil from the water surface. (i) Image of the separated water without any oil on its surface. Reproduced from ref. 30 with permission from ACS, copyright 2011.

Zhu et al. reported a simple method for removing and collecting oils and organic solvents from the water/oil mixture by using the artificial superhydrophobic and superoleophilic PU sponges.³⁰ The sponge was treated by the electroless deposition process to coat a layer of copper and subsequent chemical modification to lower surface energy via a solution-immersion step. The as-prepared sponge looked dark brown and was easily deformed by an external force such as mechanical squeezing, exhibiting good soft and elastic property (Figure 5b). The 3D configuration reveals that the sponges were rich in pores and interconnected framework (Figure 5c). The size of the micropores ranged from 200 to 450 µm. It is expected that the porous bulk structure provides a huge space for oil storage. The surface of the framework of the as-prepared sponge was covered by nanoparticles with the diameter of 100-200 nm (Figure 5d,e). The sponge could selectively absorb oils from various water/oil mixtures but repel water completely based on the synergistic effect of superhydrophobic, superoleophilic, and porous features (Figure 5f-h). The absorbed oils were easily collected by shifting the sponge to another container and a simple mechanical squeezing process, leaving only water in the original container (Figure 5i). Importantly, the recovered sponge could be efficiently reused in oil/water separation for many cycles (Figure 5a). The authors further fabricated a new kind of superhydrophobic PU sponges that are coated with Fe₃O₄ nanoparticles and dopamine.³¹ If the sponge was put on the surface of oil/water mixtures, it could quickly and selectively absorb/remove oils (e.g., lubricating oil, crude oil, and octane) from the water. Interestingly, the sponge could be easily controlled to move toward

the oil-polluted region by a magnet due to the magnetism of the Fe₃O₄ coating, Such Case Online magnetic-actuated way for oil removal is able to promote efficiency and cost savings in the process of real oil/water separation. By using the commercial melamine foams as the 3D substrate, Du et al. generated a series of rough microstructures with different dimensions on the foam surfaces via the combination of wet and dry chemical treatments (including dipping, controlled precipitation, ice-mediated coating, and annealing).³² After coating a PDMS layer, the sponge was endowed with superhydrophobicity and superoleophilicity. The as-prepared sponge exhibited great power in oil/water separation and selective oil adsorption. Cao et al. prepared superhydrophobic cotton fabrics by the processes of the deposition of a modified silica aerogel (ormosil) thin film onto the fabrics and the modification of PDMS top coating.³³ The superhydrophobicity and superoleophilicity allowed the resultant fabrics to only absorb oils but repel water. However, the poor capacity restricted the fabrics' promising application for a large volume of oil removal. To effectively avoid this problem, the authors covered the superhydrophobic fabric onto a 3D highly porous sponge with strong absorption ability and large storage capacity, forming a new oil-absorption device. This device could be applied to versatile oil/water separation with high efficiency. When the separating process was further assisted with a vacuum pump, the continuity and the speed of the separation of a large amount of oil/water mixture were greatly improved. As an ancient technology, casting refers to that a liquid material is poured into a mold, fills in the hollow cavity of the mold, and subsequently solidifies. Choi et al. used the casting method to fabricate a PDMS sponge by using the sugar as the template and using the liquid PDMS as the curing material.³⁴ After solidification of the PDMS, the sugar template was easily removed just by immersing in water, resulting in rich pores in PDMS block. The resultant PDMS sponge exhibited hydrophobic and oleophilic properties, and was very elastic. The combination of the special wettability and the porous microstructure allowed the sponge to absorb and remove oils from marine environments devastated by oil spills. Su et al. fabricated a highly porous 3D ceramic nanowire aerogel through the chemical vapor deposition method.³⁵ The aerogel was assembled by a lot of interweaving silicon carbide nanowires with the diameter of 20-50 nm and the length of tens to hundreds of micrometers. Besides the excellent refractory performance, high-temperature oxidation and heat resistance, thermal insulating property, the silicon carbide nanowire aerogel also possessed ultralow density (~5 mg cm⁻³), high porosity (99.8%), large recoverable compression strain (>70%), and remarkable fatigue resistance (more than 1000 cycles). The wettability of the aerogel was simply changed from hydrophilicity to hydrophobicity by an oil-impregnating treatment. The resultant aerogel could selectively absorb low-viscosity organic solvents on the water surface with high absorption capacity (130-237 g g⁻¹), resulting from the integrated properties of high porosity and low density. Tran et al. prepared a porous graphene-PDMS sponge through the sugar templating method. 92 The graphene sponge with hydrophobicity and oleophilicity was used for efficient oil spill clean-ups and water purification, by taking advantages of its remarkable adsorption performance for removing oils from water surface. Hayase et al. developed a method to synthesize the

superhydrophobic marshmallow-like gels, which were based on polysiloxang Article Online networks. The gels were superhydrophobic and could be used as a sponge to absorb and remove organic compounds from water. Calcagnile et al. used a solvent-free, electrostatic particle deposition method to obtain a PU foam functionalized with microscale PTFE particles and colloidal superparamagnetic iron oxide nanoparticles. The functionalized foam showed magnetic responsivity besides the water repellence and oil-absorption ability. Therefore, the resultant foam could be easily moved to the oil polluted waters by using a magnet, and selectively absorbed the floating oil from the water surface, thereby purifying the water underneath.

3. Natural superwetting materials for oil/water separation

Extreme wettability and porous microstructure are necessary to achieve effective and repeatable oil/water separation. Fortunately, lots of materials in nature and our daily life simultaneously have above two features, such as sand layer, wood sheet, and so on. Such natural superwetting porous materials are usually low-cost, eco-friendly, and can be easily obtained, which make it possible to carry out large-scale practical oil/water separating application.

3.1 Sand layer

Desert covers a vast area of the earth's surface (Figure 6a) but is uninhabitable and hard to development and exploitation. It is common knowledge that dry sands have the strong power of water absorption, which signifies that sand layer may be the superhydrophilic and underwater superoleophobic natural material and be an ideal candidate for use to separate water/oil mixtures. 102-104 Yong et al. studied the superwettability of a sand layer in air and in water and demonstrated its great ability for oil/water separation. 11 Figure 6c-e shows the SEM images of the surface of the sand particles. The sand layer exhibits a typical three-level rough microstructure (i.e., with macroscale, microscale, and nanoscale roughness). The size of the sand particles ranges from 130 to 270 µm (Figure 6c). Every sand particle has a microscale textured surface rather than a smooth surface (Figure 6d). High-magnification SEM image reveals that there are abundant nanoscale particles and debris randomly distributing on the sand surface (Figure 6e). Sand is mainly composed of silicon dioxide. In addition, it is demonstrated that sand particles also contain some metallic elements (e.g., Na, Mg, Al, K, Ca and Fe) and numerous hydroxyl groups. The effect of both high surface-free-energy compositions (silicon dioxide and metallic elements) and the hydroxyl groups leads to the inherently hydrophilic chemistry of the sand surface. When a small water droplet was dripped onto the sand layer, it would instantaneously infiltrate the sand layer within 0.03s, indicating the amazing superhydrophilic property of the sand layer. After the immersion of the sand layer in water, it exhibited quasi-superoleophobicity or superoleophobicity and ultralow oil-adhesion to a wide range of both heavy and light oil droplets, including 1,2-dichloroethane (Figure 6b,f), petroleum ether (Figure 6g), decane, dodecane, hexadecane, sesame oil, crude oil,

diesel, paraffin liquid, and chloroform droplets, as shown in Figure 7a. These 101/C8CP04009E droplets on the pre-wetted sand layer showed very high OCA values ranging from 146° to 151.5°, while all of the corresponding OSA values were smaller than 10°. The adhesive force between a 1,2-dichloroethane droplet and the sand layer was measured only to be 5.5 μN. The underwater ultralow oil-adhesive superoleophobicity is ascribed to the formation of underwater Cassie wetting state in this oil/water/sand three-phase system. The water entrapped both in the space and on the surface microstructures of the sand particles prevents the oil droplet from effectively contacting with the surface of the pre-wetted sand layer, because polar water molecules generally repel most non-polar oil molecules.

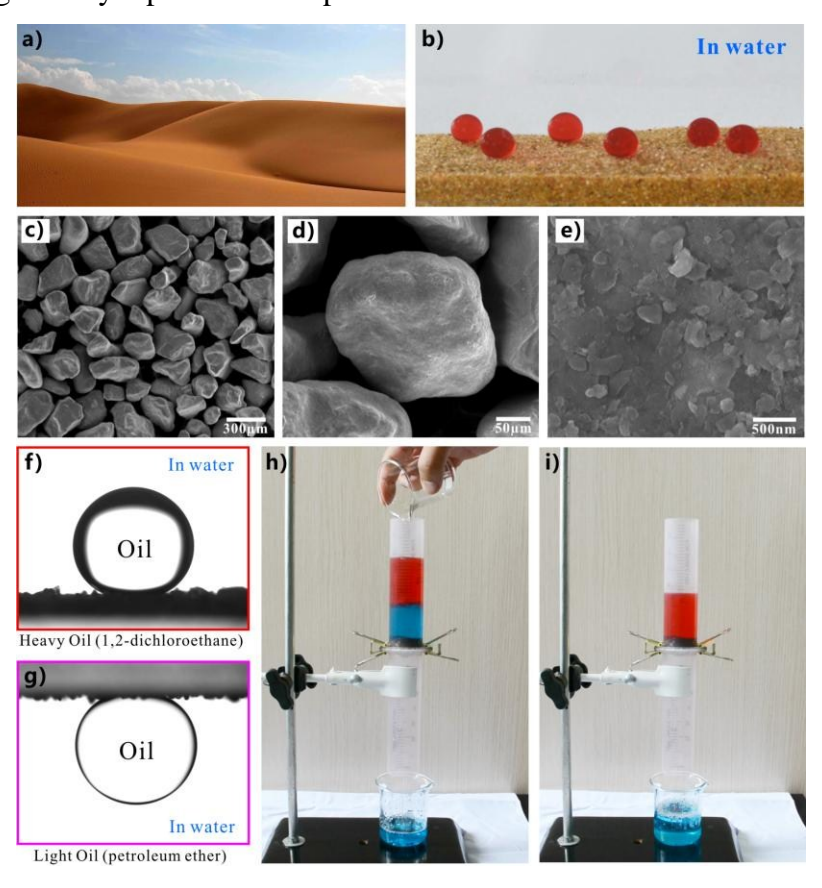


Figure 6. Oil/water separation by underwater superoleophobic sand layer. (a) Photography of the desert. (b) Oil (1,2-dichloroethane) droplets on the sand layer in a water medium. (c-e) SEM images of the surface morphology of the sand particles. (f,g) Shapes of underwater (f) heavy oil droplet (1,2-dichloroethane) and (g) light oil droplet (petroleum ether) on the sand layer. (h) Pouring the mixture of water (blue color) and oil (red color) into the designed separating device. (i) After oil/water separation. Reproduced from ref. 11 with permission from Wiley, copyright 2016.

Based on the superhydrophilicity and underwater superoleophobicity of the sand layer, an oil/water separating device was designed by using the sand layer as the core component, as shown in Figure 6h. A sand layer with the thickness of 1 cm was fixed between two bi-pass plastic tubes to act as the separating membrane, and a piece of cloth was placed below the sand layer to avoid the loss of the sand particles. Before separation operation, it was crucial to pre-wet the sand layer by pouring a small

amount of water into the upper tube. Afterward, the mixture of oil (red color, dyed/c8cp04009E with Oil Red) and water (blue color, dyed with methylene) was poured into the separating device (Figure 6h). It is obvious that the blue water quickly permeated through the waterish sand layer under the force of gravity. Instead, red oil was repelled by the pre-wetted sand layer and always stayed on the upper tube without infiltration. As a result, the mixture of immiscible oil/water mixture was successfully separated (Figure 6i), and such gravity-driving process could be repeated for many times. The separation efficiency of the pre-wetted sand layer was investigated by an optical microscope. It was found that there is almost none oil in the separated water and there is almost none water in the separated oil. The thickness of the pre-wetted sand layer had an important influence on the filtrate flux and the intrusion pressure of oil during the oil/water separation process. When the thickness of the sand layer is 0.5 cm, the water flux was about 9648 L m⁻²h⁻¹, and such layer could sustain over 39 cm of petroleum ether. With the increase of the thickness of the sand layer, the filtrate flux decreased quickly for an increased effective penetration distance, while the intrusion pressure increased because thicker sand layer led to more trapped water in the space of the sand layer. Since sand can be obtained directly from desert without any physical treatment and chemical modification, this low-cost, large-scale, green oil/water separation method has tremendous prospects in solving the problem of oil spill incident and industrial sewage drainage.

Yong et al. further put forward a novel strategy to achieve large-scale oil/water separation by using a U-shaped sand ridge. As shown in Figure 7b, the sand is piled up as a big U-shaped ridge (like a canal). The sand ridge is wetted by water in advance before separation. The top part of the sand ridge can also be wetted due to the superhydrophilicity of sand particles and the capillary action. When the mixture of water and oil is poured into the valley of the pre-wetted U-shaped sand ridge, only the water in the mixture can pass through the side wall of the pre-wetted sand ridge, whereas the oil part is intercepted by the sand ridge, thereby achieving oil/water separation. Such separation process is also spontaneous and is just driven by gravity. Moreover, this U-shaped sand ridge is able to separate the mixtures of water with not only light oils but also heavy oils.

View Article Online DOI: 10.1039/C8CP04009E

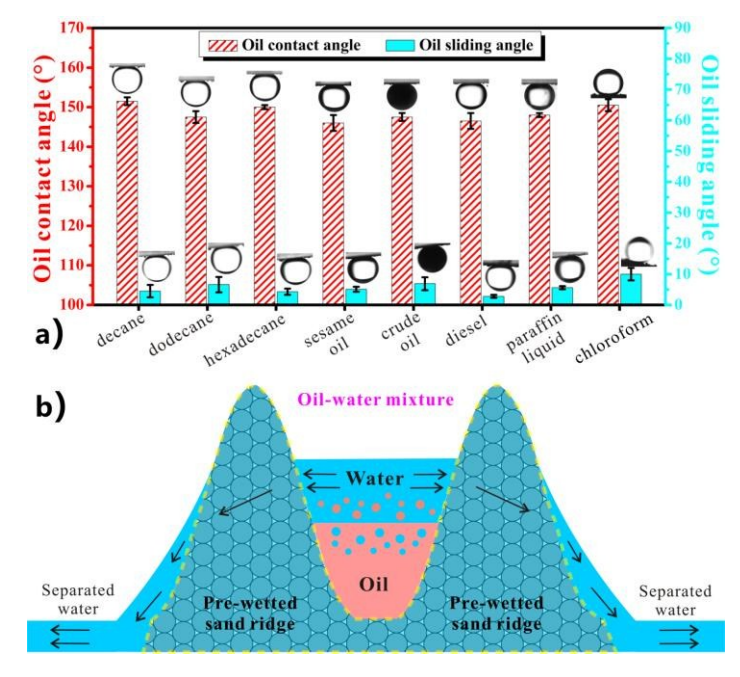


Figure 7. (a) Underwater superoleophobicity or quasi-superoleophobicity of the pre-wetted sand layer to a wide range of oil droplets. (b) Large-scale oil/water separation by using a pre-wetted U-shaped sand ridge. Reproduced from ref. 11 with permission from Wiley, copyright 2016.

Published on 17 September 2018. Downloaded by Gazi Universitesi on 9/17/2018 5:30:59 AM

Separating emulsified oil/water mixtures is also highly desirable and this process is more difficult than the separation of immiscible oil/water mixtures. 105 Such difficulty is caused by several objective reasons. On the one hand, there exist different multiple forms of emulsified oil/water mixtures, such as surfactant-stabilized and surfactant-free emulsions, oil-in-water and water-in-oil emulsions in various environments. On the other hand, the size of the numerous droplets in the emulsified mixtures is generally smaller than 20 µm. Recently, Li et al. successfully achieved the separation of various emulsified oil/water mixtures by using the sand layer. 105 The designed device is very similar to that of Yong et al. reported but without pre-wetting the sand layer (Figure 8a). 11 Because of the chemical components with high surface free energy and hierarchical rough microstructures, the sand layer showed superhydrophilicity (Figure 8b) and superoleophilicity (Figure 8c) in air. Furthermore, the sand layer also exhibited remarkable superhydrophilicity in an under-oil environment (Figure 8d). If a water droplet was dripped onto the sand layer in oil, the water would be rapidly absorbed by the sand layer. As shown in Figure 8a, the water-in-oil emulsion can be directly separated just by pouring the emulsion onto the sand layer of the designed device. It should be noticed that the sand layer does not need to be pre-wetted in this experiment. Figure 8e shows an example of separating the Span 80 stabilized water-in-diesel emulsion. The milky emulsion turned from opaque to transparent after passing through the dry sand layer (Figure 8f). From the optical microscope images, it could be found that there were a large number of packed micro-size water droplets in the original emulsion before separation (left part of Figure 8f) while no water droplets were observed in the entire image of the separated filtrate (right part of Figure 8f). Almost all of the tiny water droplets in the emulsion

were removed by the sand layer even though the droplet size is much smaller than the continuous were removed by the sand layer even though the droplet size is much smaller than the continuous continuous that the continuous continuo interspace between sand particles (Figure 8g,h). The experimental result demonstrated that the sand layer had strong separation capacity for a variety of surfactant-stabilized and surfactant-free water-in-oil emulsions, including water-in-diesel, water-in-kerosene, water-in-petroleum ether, and water-in-hexane emulsions. The separation efficiency reached up to 99.98% for the surfactant-stabilized water-in-oil emulsions and 99.99% for the surfactant-free water-in-oil emulsions. The separation efficiency increased with increasing the thickness of the sand layer, because a thicker layer results in a longer effective separation distance. The measured filtrate flux were about 400 L m⁻²h⁻¹ (stabilized water-in-diesel), 2241 L m⁻²h⁻¹ (water-in-petroleum ether), 1456 L m⁻²h⁻¹ (water-in-kerosene), and 2342 L m⁻²h⁻¹ (water-in-hexane), respectively. These values are higher than that of other filtrate materials directed only by gravity or even driven by external pressure, indicating that the sand layer had a high filtrate flux for various water-in-oil emulsions. As the thickness of the sand layer increased from 1 cm to 5 cm, the filtrate flux of water-in-oil emulsion decreased quasi-exponentially. The separation mechanism of water-in-oil emulsions via the sand layer is illustrated in Figure 8a. In general, the high-surface-energy chemical components (e.g., silicon dioxide, several metal elements, and hydroxyl groups) of sand surface endow the sand particles with stronger affinity to water than oil even in an oil-rich environment. Therefore, the surface of sand particles can easily capture micro-sized tiny water droplets from surfactant-free water-in-oil emulsions, so the water droplets impurities are extracted from the emulsions. Regarding the surfactant-stabilized emulsions, tiny water droplets and oil in the emulsions are linked by the hydrophilic and hydrophobic particles of the surfactant. Fortunately, the emulsion droplets can be easily demulsified by the sand surfaces with high surface energy because the sand particles can provide external surface energy to break the surfactant-induced force. Then, the exposed tiny water droplets are further captured and absorbed by the sand particles.

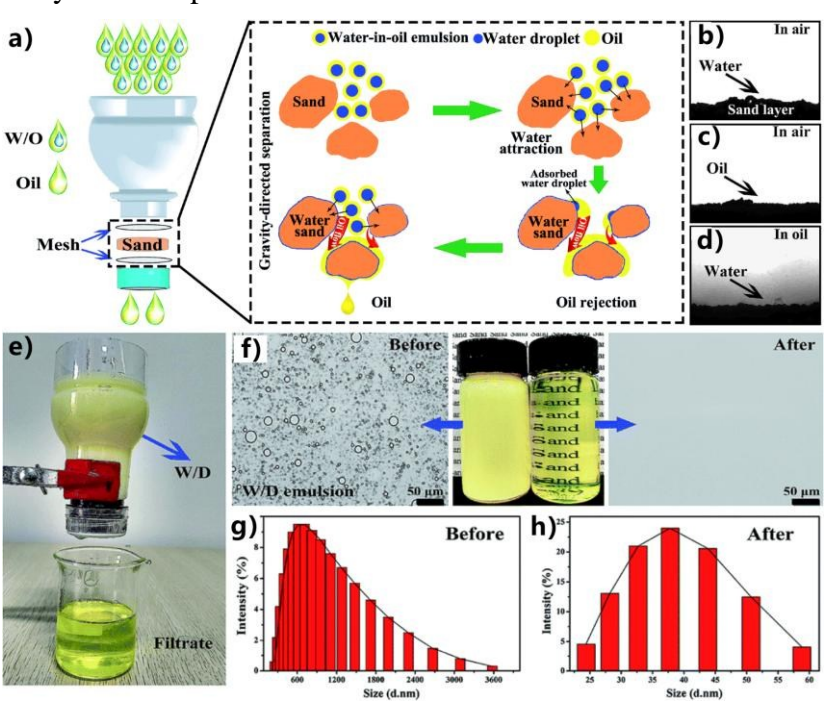


Figure 8. Separating water-in-oil emulsions by dry sand layer. (a) Schematic diagram of the separating device and colored the separating mechanism. (b-d) Wettability of different water or oil droplets on the sand layer: (b) in-air water droplet, (c) in-air oil droplet, and (d) underoil water droplet. (e) Separating the water-in-diesel emulsion. (f) Digital photographs and optical microscope images of the surfactant-stabilized water-in-diesel emulsion (left part) before and (right part) after separation. (g,h) Size distribution of the fine water droplets in (g) the original emulsion and (h) the separated filtrate, respectively. Reproduced from ref. 105 with permission from RSC, copyright 2018.

The sand particles behave like a fluid and can flow, so the sand layer must be supported by other materials to maintain its shape and prevent sand loss. Since we can get significant amounts of sands from desert, the oil/water separation based on sand layer is an inexpensive way. The sand layer is able to separate both immiscible oil/water mixtures and emulsified oil/water mixtures with an enormous volume.

3.2 Wood sheets

Dry wood is a well-known water-absorption material. The inside of the wood is composed of aligned tracheids (hollow fibers) with cell walls, forming a typical 3D hierarchical microstructure. Such 3D microstructure plays a very important role in the growth of the tree because this structure can transport water and nutrients from root to leaves. The cell walls mainly consist of cellulose nanofibrils (40%-50%, w/w), lignin (20%-30%, w/w), and hemicelluloses (20%-30%, w/w). Such hydrophilic nature and inherent porous microstructure suggest that wood may be used to separate the mixture of oil and water.

Figure 9a shows the photo of a spruce which is a major source of softwood. Figure 9b and c are the SEM images of the typical cross-section of a spruce wood. 106 Anisotropic arrangement of the softwood fibers (tracheids) can be observed. There exist two different kinds of softwood fibers on the wood cross section: the latewood (LW) region and the earlywood (EW) region (Figure 9b). The LW has thick cell walls (~25 µm) and narrow lumina (~10 µm on each side), while the EW has thin cell walls (~5 μm) and larger lumen area (~30 μm on each side). The complex wood microstructure looks like a vascular network of the living tree for fluid transport. The main wood microfeatures, lumina, and cell walls can well persevere even though the tree is felled and cut. The wood cross section surface exhibited both superhydrophilicity and superoleophilicity in air as water and oil droplets could spread out quickly on such surface and penetrate in the wood capillaries within a very short time. After the immersion of the wood sheet in water, different light and heavy oil droplets (including hexadecane, 1,2-dichloroethane, diesel, gasoline, motor oil, and olive oil) on the wood cross section surface displayed high OCA values ranging from 141° to 155°. In addition, all the measured OSAs to these oil droplets were smaller than 7°. It can be concluded that the water-soaked wood cross section shows superoleophobicity (or quasi-superoleophobicity) underwater ultralow oil-adhesion to a wide range of oils (Figure 9e,f).

As shown in Figure 9d, the underwater ultralow oil-adhesive superoleophobicity is ascribed to the formation of a stable solid/water/oil three-phase system. As the wood sheet is dipped into water, water molecules firstly penetrate the cell wall and are

bonded to hydroxyl functionalities. Then, water enters the cell lumina, leading to 3/C8CP04009E fully hydrated state. Water is trapped in the wood hierarchical microstructure and stabilized in the lumina by capillary forces, forming a thin water film on the wood surface. This trapped water layer is able to prevent the oil droplet from contacting with the wood substrate, thereby endowing the wood surface with the underwater oil-repellent property.

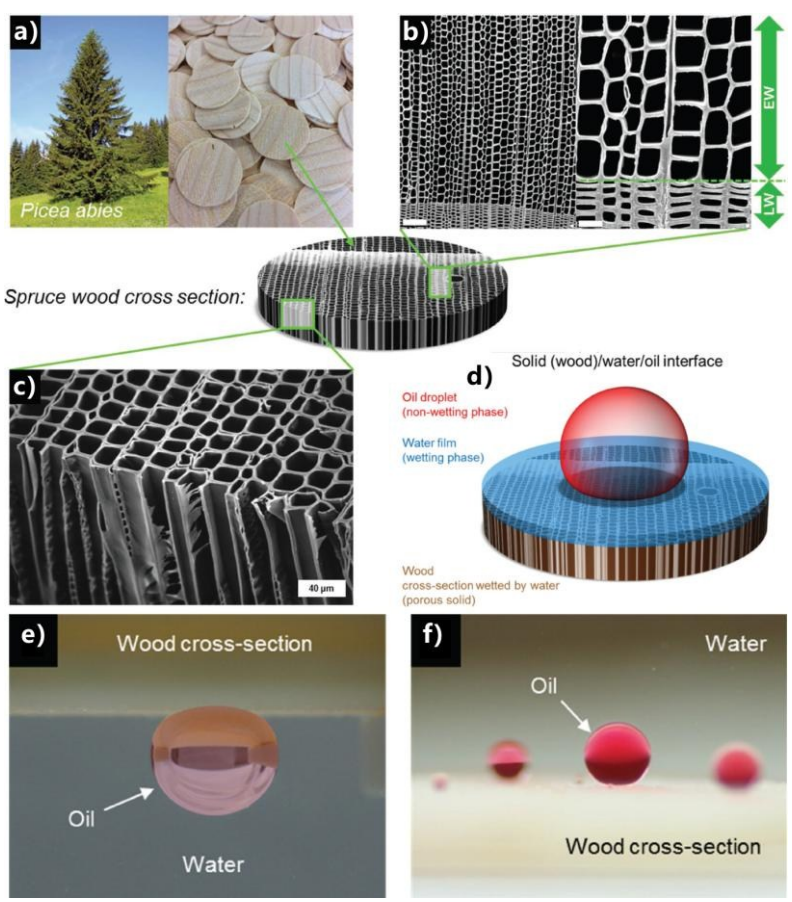


Figure 9. Microstructure and underwater superoleophobicity of the spruce wood cross section. (a) Pictures of a Norway spruce tree and the wood disks (diameter = 20 mm, thickness = 1mm). (b,c) SEM images of the wood cross section: (b) truncated tracheids from top view (left scale bar: 100 μm, right scale bar: 30 μm), (c) tracheids from a side view. (d) Schematic diagram of an underwater oil droplet on the pre-wetted wood cross section surface. (e,f) Pictures of dyed (e) light oil droplet (hexadecane) and (f) heavy oil droplet (1,2-dichloroethane) sitting on the wood surface in a water medium. Reproduced from ref. 106 with permission from Wiley, copyright 2016.

Free oil/water mixtures could be separated by using the device where the pre-wetted wood disk (with the thickness of 1 mm) was inserted between two glass tubes, as demonstrated by Cabane's group. When the mixture of hexadecane and water was poured into the upper tube, water phase would settle below the oil because of its higher density, and permeate through the wood disk quickly along the aligned tracheids. By contrast, the oil phase was intercepted above the wood disk due to the underwater superoleophobicity of the water-soaked wood surface. Therefore, water was successfully separated from the oil by this wood membrane. The porous membranes for separating immiscible oil/water mixture are usually characterized by

the separation efficiency, filtrate flux, and breakthrough pressure. The separation ($\eta = (1 - \frac{C_{\rm f}}{C_{\rm c}}) \times 100\%$) could be quantitatively calculated by analyzing the

oil contents after separation, where C_f and C_i are the oil concentration before and after separation, respectively.

The wood sheet exhibited great separating capacity with the separating efficiency for hexadecane being above 99.9%. Since wood cross sections are rich in opened structure and large pores, a very high water flux (3500 L m⁻²h⁻¹) was achieved for the wood sheet with the thickness of 1 mm. The flux decreased to 1600 L m⁻²h⁻¹ as the thickness increased to 2 mm, because of a longer fiber length in spruce wood. The breakthrough pressure is the maximum pressure that the membrane can support an oil column. When the pressure was above this threshold, oil phase may penetrate through the sheet; that is, the oil/water mixture will not be separated. The wood membrane could support a hexadecane column with a maximum height of 35 cm, corresponding to a breakthrough pressure of 2.64 kPa.

Published on 17 September 2018. Downloaded by Gazi Universitesi on 9/17/2018 5:30:59 AM

Different with the above-mentioned wood sheet that was obtained by cutting the tree in the vertical direction (perpendicular to the trunk), Yong et al. used the Balsa wood sheets that were obtained by cutting the tree along the trunk direction to achieve efficient oil/water separation. 45 The micro-pipes in the tree trunk are break and exposed when a tree is sawn into sheets, leading to abundant microgrooves on the wood surface, as shown in Figure 10a-d. The width of the grooves is only several tens microns. The wall of the microgrooves is further decorated with lots of nanoscale protrusions (Figure 10d). The wood sheet surface has excellent superhydrophilicity and underwater superoleophobicity. A uniform through microholes array was created on the wood sheet (thickness of 1mm) by a mechanical drilling process (Figure 10e). The fabricated microholes were ~340 µm in diameter and fully across from one side to another side of the wood sheet. The rest area between the microholes still kept inherent micro/nanoscale hierarchical structures (Figure 10e,f). After the immersion of the porous wood sheet in water, the optical microscope image demonstrated that the drill-induced microholes were open in water because the backlight generated from the optical microscope could successfully pass through the microholes (Figure 10g). When an underwater oil droplet was placed on the micro-holes-through wood sheet, the OCA and OSA were measured to be 155.5 $\pm 2^{\circ}$ and 7 $\pm 2^{\circ}$, respectively, revealing that the porous wood sheet still had remarkable underwater superoleophobicity after the formation of the microholes array (Figure 10h). A simple oil/water separating device was prepared by using the micro-holes-through wood sheet as the separating membrane because of its in-air superhydrophilicity and in-water superoleophobicity, as shown in Figure 10i. The wood sheet was previously wetted by a small amount of water (Figure 10j). Then, the mixture of oil (petroleum ether, red color) and water was poured into this device (Figure 10k). Water could quickly pass through the wood sheet and drip into the beaker below while oil was intercepted by the pre-wetted wood and always stayed in the upper tube (Figure 101). As a result, the mixture was successfully

separated into two parts: separated oil and separated water.

View Article Online DOI: 10.1039/C8CP04009E

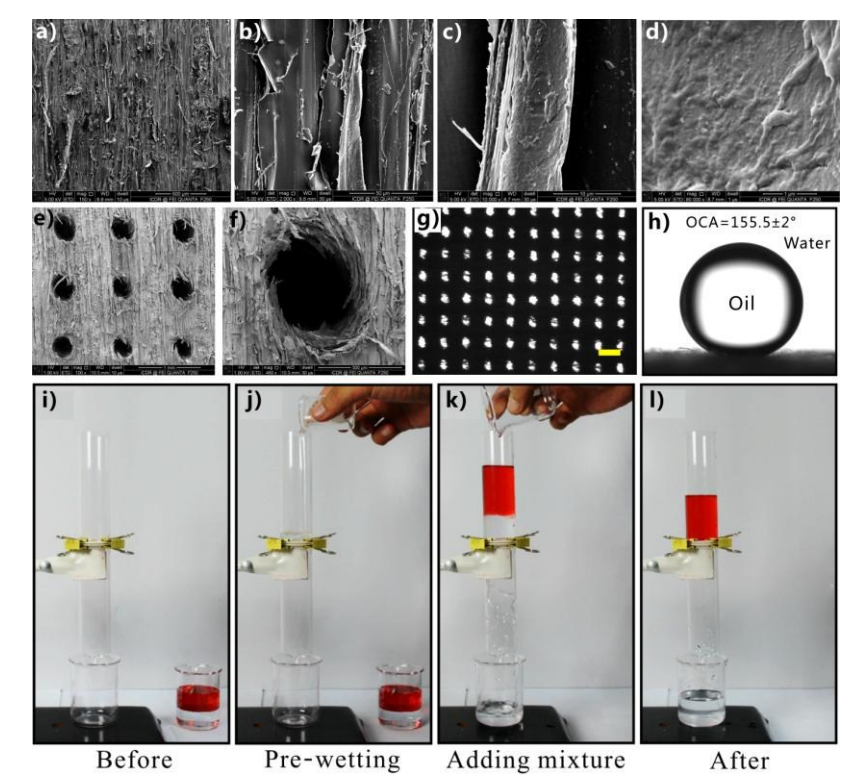


Figure 10. Separating the oil/water mixture by the micro-holes-through Balsa wood sheet. (a-d) SEM images of the wood sheet surface. (e,f) SEM images of the microholes-structured wood sheet. (g) Optical microscopy image of the micro-holes-through wood sheet in water. Scale bar = 1mm. (h) Static shape of an underwater oil droplet on the as-prepared wood surface. (i-l) A whole cycle of oil/water separation: (i) before, (j) pre-wetting the wood sheet with water, (k) pouring the mixture of oil (petroleum ether, red color) and water into the upper tube, (l) after separation. Reproduced from ref. 45 with permission from ACS, copyright 2018.

Because the oil/water separation mainly depends on the underwater superoleophobicity and porous structure of the wood surface, it is believed that most types of wood sheets can be utilized to separate the oil/water mixture. The wood has high structure strength and can be easily produced to various shapes, such as sheets, buckets, boxes, basket, and boats. Such diversity allows the wood sheets to have multiple manners for practical oil/water separation. Light wood has advantages of low density and low cost, the fabricated separating device can be easily transported to the place where oil spill occurred. Once the wood-based separating device is damaged or contaminated after a long-term work, it can be directly biodegraded by microbes in soil. A potential deterrent was that wood will swell after absorbing water; such expansion may results in the block of the artificial through-microholes or the inherent micro-channels of the thick wood sheets. Therefore, the used wood sheets should not be thick.

3.3 Nutshells

Most nut shells are green lignocellulosic biomass materials, such as coconut shell (Inset of Figure 11a). The coconut shell mainly contains plentiful amounts of

bio-degradable and nontoxic glucan, xylan, and klason-lignin with the mass /cacpo4009E percentage of 29.30%, 25.92%, and 24.36%, respectively. These chemical compositions are usually hydrophilic. Besides, the surface of the coconut shell is covered with abundant chemical or functional groups such as carboxyl, hydroxyl, amino, amide, acetamido, and so on. Li et al. obtained waste coconut shell powder (WCSP) by smashing cleaned coconut shells. 107 Figure 11a-c shows the SEM images of the surface microstructure of the WCSP. The WCSP particles present various uneven shapes (e.g., bag-like, corral-like, paper-tube-like small shapes). Those particles are randomly piled up together, leading to large empty space between the particles, with the porosity of approximate 85.80% (Figure 11a). Regarding a single particle, it exhibits a layer-by-layer packaged structure, and many apertures are found on the layer surface (Figure 11b). In addition, there are many microscale debris and nanoscale pores with the size ranging from 2 nm to 375 nm covering on the surface of the WCSP particles (Figure 11c). The WCSP layer showed both superhydrophilicity (Figure 11d) and superoleophilicity (Figure 11e) in air with CA of nearly 0° to either water droplet or oil droplet. Such superamphiphilicity has resulted from the combination of hydrophilic chemistry and hierarchical rough surface. In a liquid medium, WCSP layer exhibited underoil superhydrophilicity (Figure 11f) and underwater superoleophobicity (Figure 11g), respectively. Once a water droplet was in contact with the WCSP layer placed in oil medium, the droplet would rapidly spread out and result in a WCA of nearly 0°. In contrast, when a variety of underwater oil droplets were positioned onto the WCSP layer, all of the oil droplets could maintain spherical shapes with OCA ranging from 155 ° to 163 °. The WCSP layer also had very low underwater oil-adhesion because those oil droplets were able to roll off a 5 °tilted WCSP layer freely.

The excellent underwater superoleophobicity ensures that the WCSP layer can potentially be used as filtrate membrane for separating various immiscible oil/water mixtures. As shown in Figure 11h, when the mixture of diesel (dyed with Oil Red O) and water (dyed with methylene blue) was poured onto the pre-wetted WCSP layer, the blue water would instantly start to permeate through the layer. It should be noticed that the separated water in the beaker was colorless because the methylene blue dye was fully absorbed by the WCSP particles. Finally, the diesel was retained on the layer due to the great underwater superoleophobicity of the WCSP layer after the water in the mixture being completely removed. In the same way, other immiscible mixtures of water and various oils such as kerosene, petroleum ether, hexane, toluene, and heptane were also successfully separated by the pre-wetted WCSP layer. The oil contents in the filtrates of various oil/water mixtures after separation were less than 70 ppm, implying that the separation efficiency reached up to 99.99% for a series of oil/water mixtures. In addition, the separating device using the WCSP layer as the core component had great recyclability since the separation efficiency still maintained above 99.98% even after 50 cycles of separation.

View Article Online DOI: 10.1039/C8CP04009E

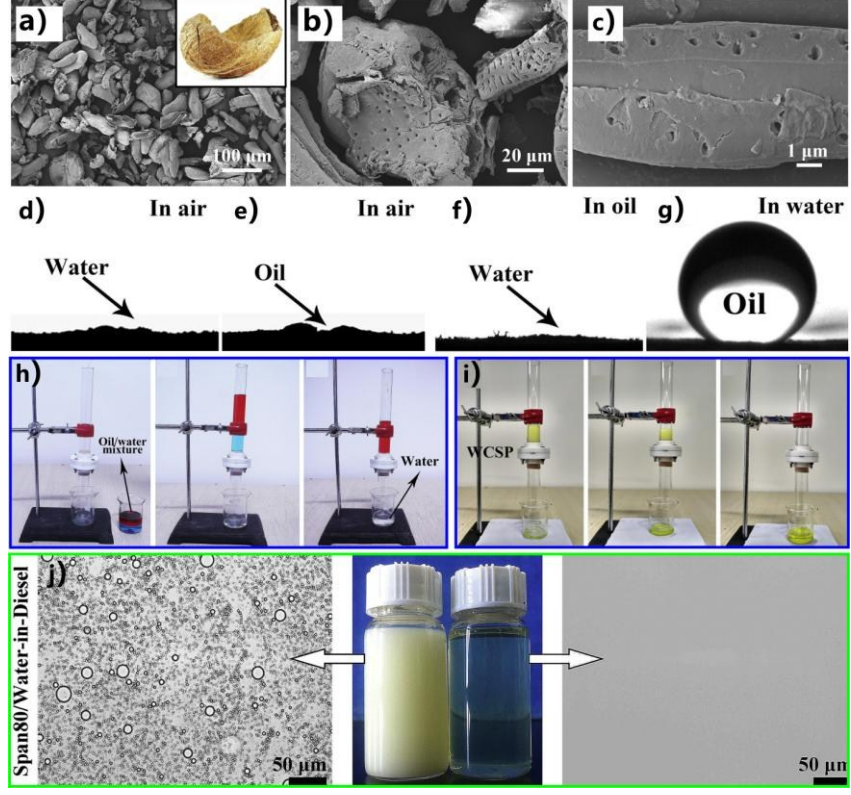


Figure 11. Separating immiscible oil/water mixture and water-in-oil emulsion by using waste coconut shell powder layer as the filtrating membrane. (a-c) SEM images of the surface of the WCSP particles. (d-g) Wettability of different water or oil droplets on the WCSP layer: (d) in-air water droplet, (e) in-air oil droplet, (f) underoil water droplet, and (g) underwater oil droplet. (h) Separation process of an immiscible oil/water mixture. (i) Separation process of a water-in-oil emulsion. (j) Optical microscopy images of the water-in-oil emulsion before (left part) and after (right part) separation. Reproduced from ref. 107 with permission from Elsevier, copyright 2018.

Apart from the immiscible oil/water mixtures, the WCSP layer also can separate various water-in-oil emulsions by taking the advantage of the underoil superhydrophilicity and the special porous microstructures of the WCSP particles. 107 As shown in Figure 11i, after the Span 80 stabilized water-in-oil emulsion being poured onto the layer, all the emulsions could easily be separated with high separation efficiency (99.98%). The collected filtrate was transparent rather than the milky color of the original water-in-diesel emulsion. Figure 11j shows the optical microscopy images of the mixture before and after separation. It can be seen that there are plenty of densely packed water droplets in the original emulsion (left) while there is no single water droplet in the filtrate (right). Further research demonstrated that the tiny water droplets in the emulsion were also completely removed by the WCSP particles. Different from most of the special-wetting materials that separate the water-in-oil emulsions based on the "size-sieving" effect, in fact, the WCSP layer achieves emulsion separation via an "adsorption" effect. There exist many polar hydrophilic functional groups such as carboxyl, hydroxyl groups on the WCSP surface. Therefore, stronger intra- and inter-molecular hydrogen bonding can easily form, which endows the surfaces of WCSP with stronger tendency to capture tiny water droplets from the

polar water-in-oil emulsion because hydrogen bonding has a stronger affinity to water-in-oil emulsion is poured onto the WCSP layer, the emulsified water droplets will be quickly demulsified and then adsorbed by the WCSP particles, only allowing the purified oil to permeate through the separating layer by gravity.

Li et al. also used walnut shell powder (WSP) to achieve gravity-driven oil/water separation. 108 The walnut shell is made up of most typical hydrophilic substances including lignin and cellulose which are rich in active groups (-OH and _COO⁻). Walnut shell was firstly crushed into powder and dried. And then, the powder was further passed through a 40 mesh sieve to obtain fine WSP particles with the size of 60-300 µm. In addition to the large empty spaces among the particles, a microscale rough structure is also exhibited by the surface of the particles. Due to the hydrophilic chemical composition, remarkable water absorption capacity, and the hierarchical rough microstructures, the WSP layer had excellent superoleophobicity and ultralow oil-adhesion to various small oil droplets in a water medium. A pre-wetted WSP layer with the thickness of 1 cm was simply sandwiched between a beverage bottle and its bottle cap to act as a separating membrane. When the mixture of water and diesel was poured into the device, the water phase in the mixture immediately permeated through the WSP layer because of the superhydrophilicity, whereas the diesel was intercepted by the layer. The separation efficiency of the WSP layer reached up to 99.94% for various oil/water mixtures. In addition to the high efficiency of separating the immiscible oil/water mixtures, the WSP layer also had excellent adsorbing property to the organic dyes (e.g., methylene blue, crystal violet, rhodamine B) in a water phase. The WSPs layer was able to effectively remove dyes from water with the decolorization rate above 99.2%.

The waste nutshell is green, low price, nontoxic, renewable and easily obtained. Furthermore, the nutshell is usually one of the sources of worldwide pollutant to environment. The conversion of the waste nutshell into a desired oil/water separating material not only creates a unique way to cope with oil quality deterioration but also reduces the pressure on the environment.

3.4 Waste potato residue-coated mesh

Published on 17 September 2018. Downloaded by Gazi Universitesi on 9/17/2018 5:30:59 AM

Li et al. reported a waste potato residue powder (PRP) coated mesh with robust underwater superoleophobicity and underoil superhydrophobicity by spraying the mixture of PRPs and waterborne PU onto a stainless steel mesh. ¹⁰⁹ PRP is a typical superamphiphilic material because it consists of massive superhydrophilic and superoleophilic substances such as starch, cellulose, and pectin. The PU was used to increase the binding force between PRPs and the mesh. Compared to the flat surface of the original mesh (Figure 12a), the as-prepared PRPs-coated mesh exhibited hierarchical rough morphology with the spherical or irregular PRPs aggregating on and attaching to the mesh surface closely (Figure 12b,c). Combining with the inherent amphiphilic property of PRPs, the textured mesh simultaneously showed superhydrophilicity (Figure 12d) and superoleophilicity (Figure 12f) in air. Once the mesh was immersed in water, water would wet and be trapped in the rough

microstructures of the mesh to form a water/solid interface. When an oil (kerosene //cacpo4009E droplet was placed on such underwater mesh, the mesh showed underwater superoleophobicity to the oil droplet with the OCA of 152° due to the strong repellence of the tapped water layer (Figure 12e). Similarly, in the oil (kerosene) medium, the mesh showed underoil superhydrophobicity to a water droplet with WCA larger than 150 ° due to the repellence of the tapped oil layer (Figure 12g). The further experiment indicated that the as-prepared mesh could exhibit superoleophobicity to a series of oil droplets in water, such as kerosene, rapeseed oil, petroleum ether, hexane, and chloroform. Correspondingly, the mesh also exhibited (super-) hydrophobicity to a small water droplet in various oils with WCA larger than 140°. The special wettability of the PRPs-coated mesh could be used to selectively remove water or oil from the oil/water mixtures depending on whether the oil is heavier than water or not, as shown in Figure 12h. For the case of the mixture of light oils and water (ρ_{water} > ρ_{oil}), the mesh needed be pre-wetted by water in advance to obtain underwater superoleophobicity. Such mesh was able to selectively remove water from an oil/water mixture. When the mixture was poured into the separating device, the water in the mixture was able to permeate through the mesh while the oil was intercepted by the mesh (Figure 12h,i). Regarding the mixture of water and heavy oils ($\rho_{\text{water}} < \rho_{\text{oil}}$), the mesh needed to be pre-wetted by oil in advance to obtain underoil superhydrophobicity. Such mesh was able to selectively remove heavy oil from an oil/water mixture. When the mixture was poured into the separating device, the oil in the mixture could permeate through the mesh while the water was intercepted by the mesh (Figure 12h,j). Such selective separation process showed high separation efficiency and stable recyclability. The efficiency was higher than 96.5% for separating various light or heavy oil/water mixtures. The separation efficiency remained above 98.0% after 40 recycle numbers of separating kerosene/water mixture. In addition, the potato residue-coated mesh also could be used to separate the mixtures of oil and different corrosive water solutions (such as 1 mol L⁻¹ HCl, 1 mol L⁻¹ NaOH, and 10 wt% NaCl).

View Article Online DOI: 10.1039/C8CP04009E

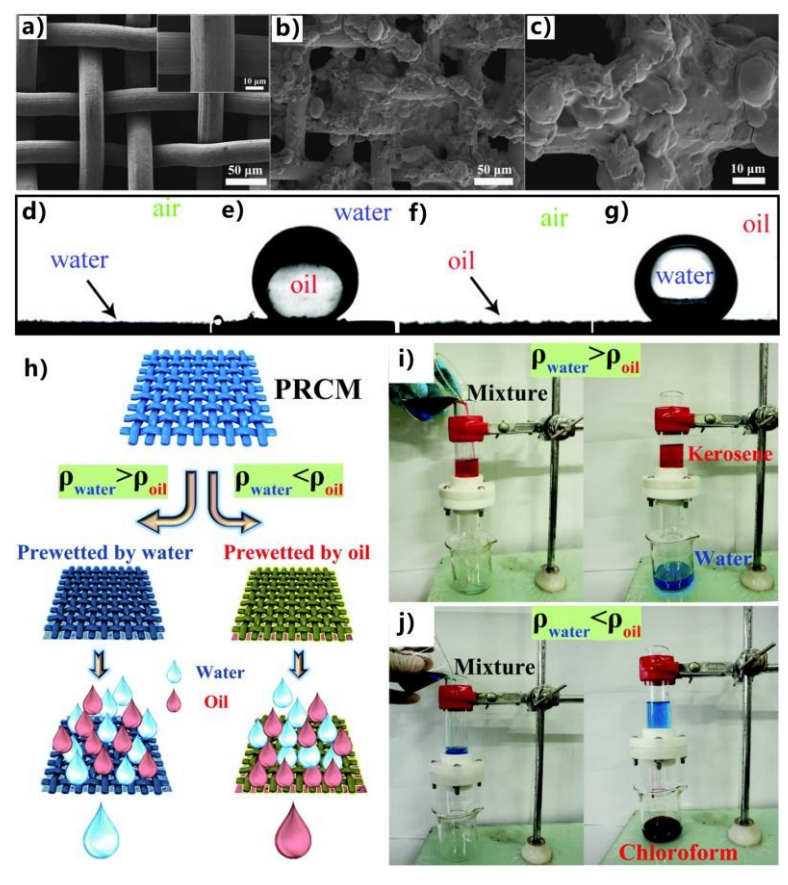


Figure 12. Selective oil/water separation based on the potato residue powder-coated mesh. (a) SEM image of the bare flat stainless steel mesh. (b,c) SEM images of the potato residue powder-coated mesh. (d-g) Wettability of different water or oil droplets on the PRPs-coated mesh: (d) in-air water droplet, (e) underwater oil droplet, (f) in-air oil droplet, and (g) underoil water droplet. (h) Schematic diagram of the process of selective oil/water separation. (i) Separating the mixture of water and light oil by using a water-wetted PRPs-coated mesh. (j) Separating the mixture of water and heavy oil by using an oil-wetted PRPs-coated mesh. Reproduced from ref. 109 with permission from RSC, copyright 2016.

Published on 17 September 2018. Downloaded by Gazi Universitesi on 9/17/2018 5:30:59 AM

The water/oil separation mechanism of the PRPs-coated mesh is shown in Figure 13. If the mesh is hydrophobic or oleophobic (the water or oil contact angle $\theta > 90^{\circ}$), the breakthrough pressure is positive value ($\Delta P > 0$), so the mesh can sustain a certain pressure (negative capillary effect). Only when an external pressure is applied, the water and oils can spontaneously penetrate through the mesh. On the contrary, when the mesh is hydrophilic or oleophilic ($\theta < 90^{\circ}$), the breakthrough pressure is negative value ($\Delta P < 0$), so the mesh cannot withstand any pressure (capillary effect). The liquids are able to permeate the mesh spontaneously. The PRPs-coated mesh shows both superhydrophilicity and superoleophilicity in air, so $\Delta P < 0$, revealing that the as-prepared mesh cannot support any pressure (Figure 13ab). When the water or oils are poured onto such mesh, they will penetrate through the mesh spontaneously, driven by the hydrophilic/oleophilic force and gravity. Once the rough mesh is pre-wetted by water, the hierarchical microstructures on the mesh surface are occupied by water. After oils being poured onto the mesh, the oils are repelled by the mesh due to the repellent force provided by the water layer around the mesh surface. θ

is obviously larger than 90 ° and Δ P > 0, so the pre-water-wetted mesh could support (C8CP04009E) oil pressure to some extent (Figure 13c). Similarly, it can be inferred that the pre-oil-wetted mesh could support water pressure to some extent (Figure 13d). Therefore, it is clear that the superhydrophilicity and superoleophilicity allow the wetting phase (water or oil) to quickly penetrate through the PRPs-coated mesh, whereas the non-wetting phase is intercepted above the mesh by the underwater superoleophobicity or underoil superhydrophobicity. As a result, the as-prepared mesh can separate various kinds of light or heavy oil/water mixtures by selectively using the underwater superoleophobic or underoil superhydrophobic properties.

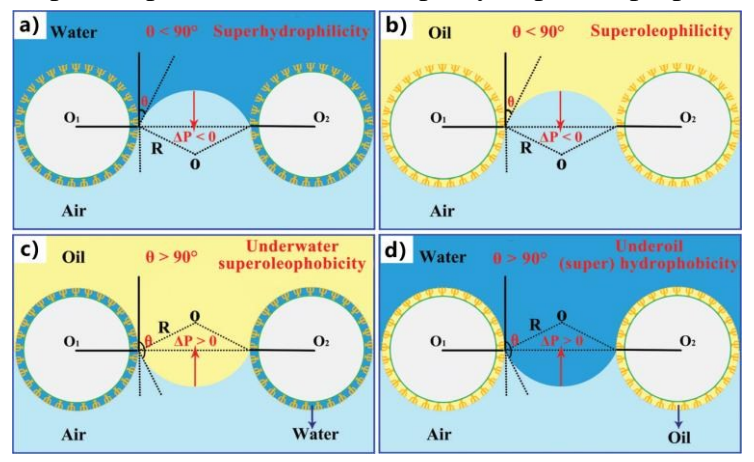


Figure 13. Schematic diagrams of selective oil/water separation by using the potato residue powder-coated mesh. (a) Water and (b) oil can penetrate through the superhydrophilic and superoleophilic mesh in air, because $\Delta P < 0$. (c) Oil cannot penetrate through the pre-water-wetted mesh, because $\Delta P > 0$. (d) Water cannot penetrate through the pre-oil-wetted mesh, because $\Delta P > 0$. Reproduced from ref. 109 with permission from RSC, copyright 2016.

The single superhydrophobic membrane is suit to separate the mixture of heavy oils and water, while the single underwater superoleophobic membrane is suit to separate the mixture of light oils and water. It can be found that both of such two separating films are not universally applicable. Each separating material is only suitable for a certain case. Interestingly, the PRPs-coated mesh that integrates with underwater superoleophobicity and underoil superhydrophobicity can separate both light oil/water mixtures and heavy oil/water mixtures. The underwater superoleophobicity endows the water-wetted mesh with the ability to separate the mixture of water and light oils, while the underoil superhydrophobicity allows the oil-wetted mesh to separate the mixture of water and heavy oils.

3.5 Diatomite membrane

Diatom is a kind of unicellular photosynthetic microalgaes which are a major group of microorganisms found in the oceans, waterways and soils of the world and play an important role in the eco-system. The complete diatom frustules are cylindrical in shape, with the diameter of 5-15 µm and the height of 10-15 µm (Figure 14a). There are also many ordered nano-holes on the wall of the diatom frustules. The skeleton of diatom is composed of hydrated amorphous silica. Lo et al. prepared the diatomite membranes with hierarchical microstructures by using the freeze casing technique. ¹¹⁰

The diatomite slurry consisting of diatomite powder, organic binder and nionis / C8CP04009E dispersant was poured into a tube. Under a unidirectional cooling flux, the ice crystals solidified. Meanwhile, the lamellar structures were formed, with expelling diatomite within the slurry. The ice template was then removed through a sublimation process (with increasing temperature). As a result, the diatomite scaffold with the synthesized lamellar microstructures was obtained. Figure 14b shows the morphology of the transverse section of the as-prepared diatomite membrane. The diatomite membrane is rich in elongated micro-channels and nano-porous structures. For the membrane prepared with the cooling rate of 5 °C min⁻¹, the size of the channels is ~15 µm in short axis and ~30 µm in long axis. Chemical analyses indicated that the diatomite membrane is mainly made up of silica and aluminosilica, which are inherently hydrophilic. The resultant membrane had both superhydrophilicity superoleophilicity in air. When the membrane was immersed in water, it showed superoleophobicity against oils and various organic alkanes, with the OCA of 169.4° for soybean oil (Figure 14c), 167.1° for hexane, 167.0° for hexadecane, 168.3° for dodecane, 170.2 ° for light crude oil, and 171.1 ° for heavy crude oil. Even though the membrane was immersed in 1 M HCl solution, sea water, and artificial sea water for 24 hours, no decrement of the OCA values was observed, demonstrating excellent oil repellency of the membrane under harsh environments (Figure 14c). Remarkable capacity for separating oil/water mixture by the diatomite membrane was demonstrated. A pre-water-wetted diatomite membrane with the thickness of 2 mm was fixed between two glass tubes. When the oil/water mixture was poured into the upper tube, the membrane only allowed the water to penetrate through but the oil was intercepted in the upper tube, because of the superhydrophilicity and underwater superoleophobicity of the pre-wetted membrane. The porous diatomite membrane could separate various free oil/water mixtures with the efficiency above 99.5%, even under acidic and briny environments (Figure 14d). The water flux during the separation was about 6602 L m⁻²h⁻¹. The measured intrusion pressure was 7.2 kPa because the diatomite membrane could support an oil column (soybean oil) with the height of 80 cm. After 30 cycles of separation, the diatomite membrane still maintained its strong underwater oil repellency (Figure 14e). The pre-wetted diatomite membrane was immersed into soybean oil bath for certain period of time, and then it was taken out and flushed by water. It was found that long-term immersion into oil bath did not weaken the underwater superoleophobicity of the membrane (Figure 14f). Such durability of the diatomite membrane is important for the long-term oil/water separation.

View Article Online DOI: 10.1039/C8CP04009E

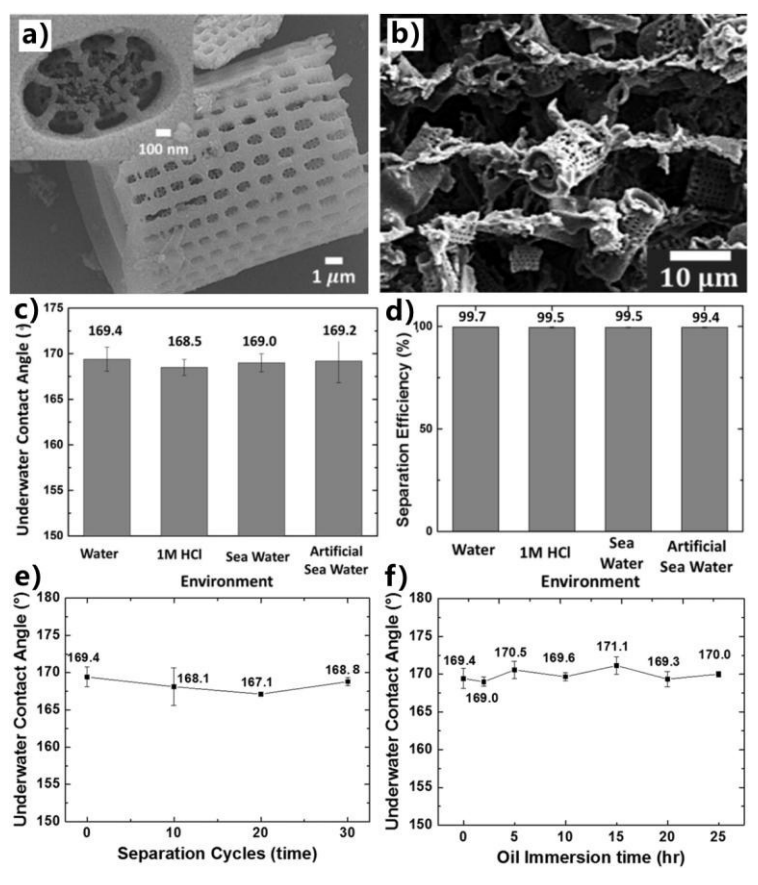


Figure 14. Separating free oil/water mixture by using the diatomite membrane as the filtrating membrane. (a) SEM images of the hierarchical microstructure of a single diatom frustule. The inset shows the high-magnification nano-holes on the silica frustule. (b) Microstructure of the as-prepared diatomite membrane. (c) Oil contact angle of an oil droplet on the diatomite membrane in different aqueous solutions. (d) Efficiencies of separating the mixtures of oil and different aqueous solutions. (e,f) Underwater superoleophobicity of the diatomite membrane after (e) different cycles of oil/water separation and (f) immersing in a soybean oil bath for a period of time. Reproduced from ref. 110 with permission from Springer Nature, copyright 2017.

3.6 Cotton ball

There are many kinds of fibrous substrates in nature, such as the cotton ball. Manna et al. used the fibrous cotton to collect/clean oils from different forms of oil-contamination, including floating light-oil, sedimentary heavy-oil, and emulsions (Figure 15). To endow the cotton with both superhydrophobicity and superoleophilicity, the cotton was treated by a scalable and eco-friendly dip-coating method. The cotton was firstly functionalized with branched polyethylenimine and then coated with 'amine-reactive' nanocomplex. After further modification of the nanocomplex-coated cotton with octadecylamine molecules through a 1,4-conjugate addition reaction, the resultant materials exhibited great ability to repel water both in air (Figure 15a) and under oil (Figure 15c). The advancing CAs of a small water droplet in air and in water were 161 ° (Figure 15b) and 163 ° (Figure 15d), respectively. When the superhydrophobic cotton was submerged in water, a shiny reflection appeared at the solid/water interface, surrounding the bulk cotton (Figure 15e). This result indicated that air was trapped in the microstructure of the cotton, and this

simple study eventually revalidated the existence of a stable Cassie wetting state of cassie wetting s the material. However, oils were easily absorbed by the as-prepared cotton, with an OCA of 0°. The contrasting surface wettability of the cotton to water and oil provided a simple basis to separate oil through both selective absorption and filtration processes. The as-prepared superhydrophobic cotton was proven to separate bulk oil/water mixtures through absorption-based selective oil collection, irrespective of the density of the oils and their locations (both above and under the aqueous phase). In a real environment, oil contaminants are either floating on the air/water interface (light oils) or are sediments on the beds of the sea, lake, and river (heavy oils). As shown in Figure 15g, when a piece of the superhydrophobic cotton ball was in contact with an oil/water mixture consisting of water and floating motor oil (light oil), the motor oil would be rapidly soaked into the cotton but the cotton could not absorb any water. In addition, the oil-soaked cotton was able to always float on the top of the aqueous phase. By a similar absorbing principle, the superhydrophobic cotton also could remove sedimentary heavy oils from the oil/water mixture, such as the mixture of model-oil (heavy oil) and water (Figure 15h). The sedimentary oil was instantly absorbed by the cotton after exposing the cotton to the oil phase underwater, while no trace of water was noticed in the cotton. Regarding the mixtures of water and different oils (e.g., chloroform, dichloromethane, silicone oil, ethyl-acetate, motor oil, and kerosene oil), the synthesized superhydrophobic cotton showed the separation efficiency above 97% and an absorption capacity above 2000% (with respect to the mass of cotton), irrespective of the density and chemical composition of the oils. Furthermore, even the water-in-oil emulsion could be separated by the device that was made up of superhydrophobic cotton, as shown in Figure 15i-l. When the turbid emulsion was poured into the separating device, the oil droplets were selectively filtered through the cotton and instantly separated from the aqueous phase (Figure 15i,j). The micro water droplets (Figure 15k) that existed in the emulsion solution were not observed in the oil phase after performing the separation process (Figure 151). Around 95% of oil in the emulsion was successively collected even after the superhydrophobic cotton being repeatedly used for 100 times. The resultant superhydrophobic cotton could even efficiently separate oil from aqueous phases that are chemically harsh (including extremes of pH = 1 & 12, artificial seawater, etc.), and could maintain its separating ability even after prolonged exposure to UV irradiation for 10 days and after incurring various physical deformations.

View Article Online

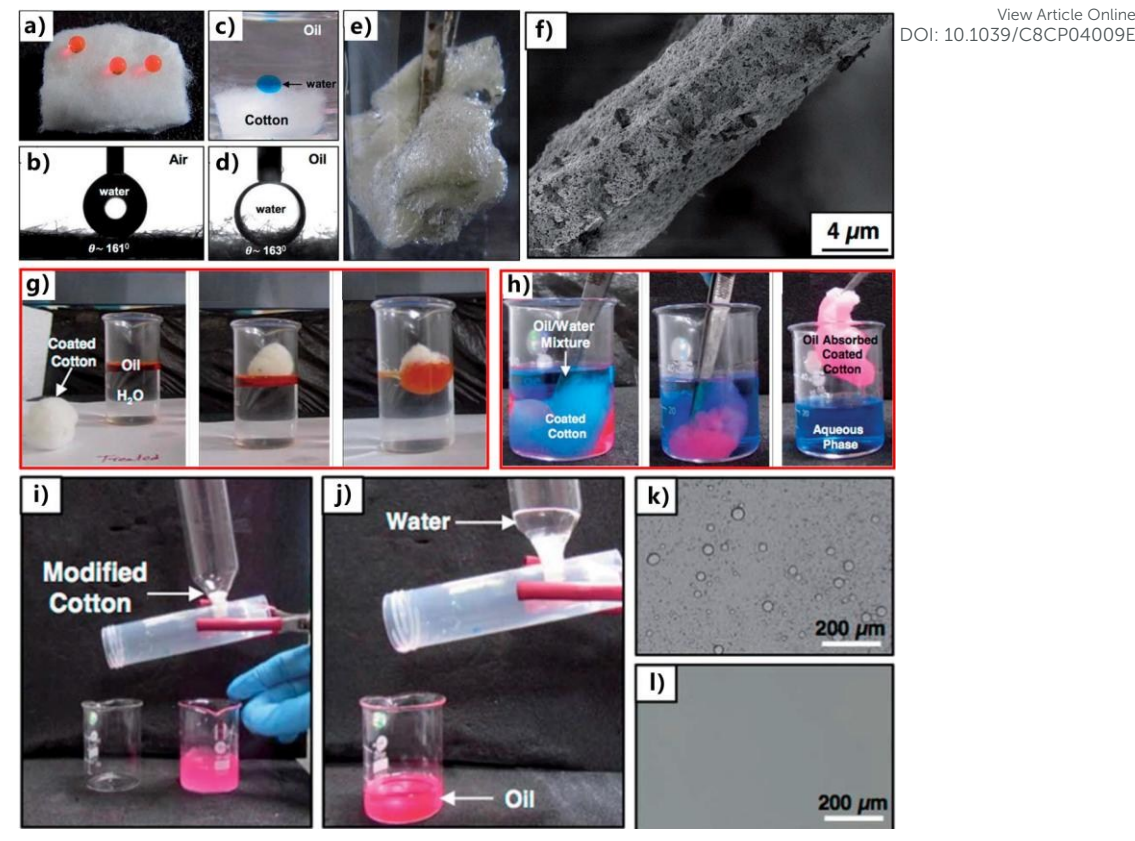


Figure 15. Using the as-prepared superhydrophobic cotton to separate oil from different forms of oil-contamination, including floating light-oil, sedimentary heavy-oil, and emulsions. (a,b) Water droplets on the cotton surface in air. (c,d) Water droplet on the cotton surface underoil. (e) Photography of a piece of an as-prepared cotton ball in the water. (f) SEM image of the nanocomplex-coated cotton. (g) Removing floating motor oil (red color) from water surface by using the as-prepared cotton. (h) Removing sedimentary model-oil (heavy oil, red color) under water (blue color) from the oil/water mixture by using the as-prepared cotton. (i-l) Separating the water-in-oil emulsion by using the as-prepared cotton. Reproduced from ref. 111 with permission from RSC, copyright 2017.

It is very difficult for the superhydrophobic or underwater superoleophobic 2D membrane to address the oil-polluted water like a small amount of oil being leaked to sea surface and the case of leaked heavy oils on the seafloor. Fortunately, the superhydrophobic/superoleophilic cotton can solve these special cases by directly absorbing and removing oils from water based on an absorption way.

3.7 Dandelion seeds

Dandelion seed (Figure 16a) is composed of an achene, a beak, and a radial array of 84-96 feathery/white fibers (i.e., pappi). The length of the fibers ranges from 4.65 to 5.90 mm. The fibers radially distributing around the beak are absolutely vital for the dandelion's multiply as they can collect rain droplets to aid seed germination and take the dandelion seeds to find the best living environment. 113 The diameter of the fibers is about 20 µm (Figure 16b). There are some sharp-tipped spikes with a length of ~19.9 µm further distributing along the fibers (Figure 16c,d), which can enhance the interaction between the fibers and liquid. The fibers showed hydrophobicity with

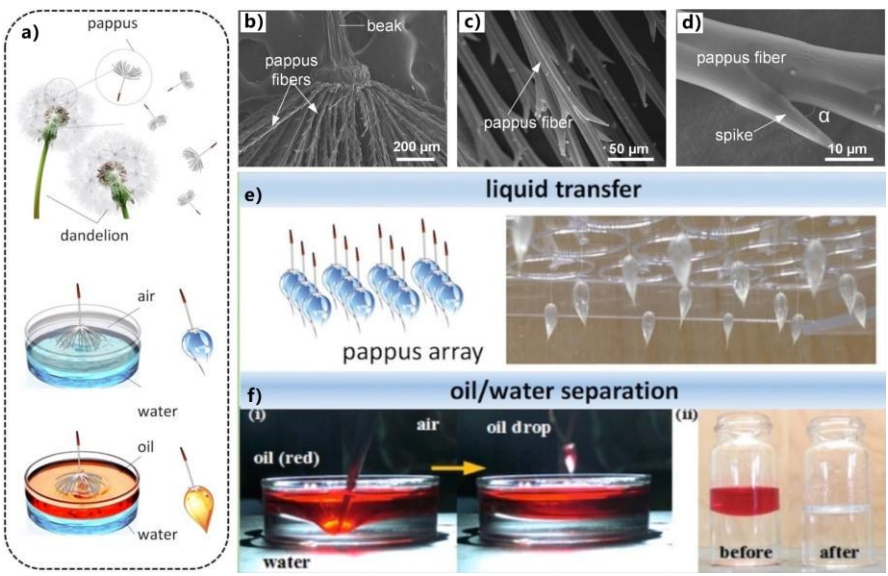


Figure 16. Liquid-transferring ability of dandelion seeds. (a) Schematic diagram of a dandelion seed (top image), capturing a water droplet (middle image), and capturing an oil droplet (bottom image) by a dandelion seed. (b-d) SEM images of the microstructure of the fibers. (e) Parallelization of the fiber assays for improving liquid transport capacity. (f) Transferring oil droplets from the mixture of water and light oil by using dandelion seeds. Reproduced from ref. 112 with permission from Wiley, copyright 2017.

The liquid-transferring ability of dandelion seeds can be utilized for oil/water separation by removing one liquid phase away from the mixture. Figure 16f shows an example of separating the mixture of layered water and light oil (red color). After the immersion of the dandelion seeds in the mixture, the fiber assay would be wetted by the upper oil phase. When the dandelion seeds were taken out of the mixture, oil droplets were encapsulated inside of every fiber assay and could be removed away. The mixture was completely separated by continually repeating the transfer process.

Because the volume of the transferred oil by the dandelion seed is limited for every transport, the oil/water separation based on the radical fiber assay is more suitable for the case that little oils float on water surface. In addition, the reusability of the dandelion seed should be improved in practical applications.

View Article Online DOI: 10.1039/C8CP04009E

4. Conclusions and outlook

The frequency of oil-spill accidents and the increasing amount of industrial wastewater discharges have caused severe water pollution, not only resulting in huge economic losses but also threatening the ecological system. Recently, many materials with special wettability (such as superhydrophobicity or superoleophobicity) have been developed to achieve effective oil/water separation. However, the cost of the adopted materials, the expensive equipment, and the complicated process for endowing those materials with special wettability become a tremendous burden for large-scale application of oil/water separation. This review introduces the recent developments of oil/water separation by using natural superwetting materials. For every kind of natural materials, we briefly show how to use them to separate a mixture of water and oil, including the inherent superwettability of the natural porous materials, separating method/process, and separation mechanism. Because the natural superwetting materials are usually low-cost, eco-friendly, and can be easily obtained, so the oil/water separation based on those natural materials is a better choice to address above-mentioned globally recognized oil contamination challenge.

Although the natural superwetting materials have been successfully applied in oil/water separation and show great separating performance, there are still many challenges in this field, and some of the problems still need to be solved before the natural materials being used in the practical treatment of oil spill accidents and industrial oily wastewater. Firstly, the reported superwetting materials in nature and our daily life that have remarkable oil/water separating ability are still limited. Nature is colorful; therefore, more such natural separating materials are being discovered in coming years. Secondly, more qualitative and quantitative study is required to further understand the interactions between the porous superwetting materials and oil/water mixtures. For example, it is still less well known how do the oil/water mixtures interact dynamically with a superwetting surface during the separation process. When a superhydrophobic/superoleophilic surface is in contact with oil, the surface will become an oil-infused surface in fact and may partly or even completely lose its superhydrophobicity in theory. Similarly, in the separating process by using an underwater superoleophobic material, the separated oils are usually on the material surface rather than under water. The fundamental theory plays a very important guiding role in using the natural materials to achieve efficient oil/water separation. Thirdly, in most reported separation experiments, researchers usually used a pure oily liquid as the oil contaminant and the model oil, but the pure oils are very different from the oil pollutant in the true situation of an oil-spill accident. In some cases, the real oil pollutant has a high viscosity and high density, which will weaken the separation ability and efficiency of the material surfaces substantially because of no matter the fouling of the separating materials or the damage of the pore structure and special wettability of the substrate. The technology of separating the mixture of water and high-viscous oils should be developed. Finally, and perhaps most importantly,

Physical Chemistry Chemical Physics Accepted Manuscript

although many natural superwetting materials have been proved to have more more cost, green, large-scale, advantages than common artificial separating materials in low-cost, green, large-scale, sustainable oil/water separation, those materials have still been not moved from the laboratory to the market until now. In the future, researchers should attempt to apply the natural separating materials in a real environment to practically solve the pollution problems caused by oil spills and oily industrial wastewater.

Conflicts of interest

There are no conflicts to declare.

Acknowledgements

This work is supported by the National Key Research and Development Program of China under the Grant no. 2017YFB1104700, the National Science Foundation of China under the Grant nos. 51335008, 61875158, and 61805192, the NSAF Grant No. U1630111, China Postdoctoral Science Foundation under the Grant no. 2016M600786, the Collaborative Innovation Center of Suzhou Nano Science and Technology, and the International Joint Research Laboratory for Micro/Nano Manufacturing and Measurement Technologies.

References:

- [1] Z. Xue, Y. Cao, N. Liu, L. Feng and L. Jiang, *J. Mater. Chem. A*, 2014, **2**, 2445-2460.
- [2] B. Wang, W. Liang, Z. Guo and W. Liu, Chem. Soc. Rev., 2015, 44, 336-361.
- [3] Z. Chu, Y. Feng and S. Seeger, Angew. Chem. Int. Ed., 2015, 54, 2328-2338.
- [4] R. K. Gupta, G. J. Dunderdale, M. W. England and A. Hozumi, *J. Mater. Chem. A*, 2017, **5**, 16025-16058.
- [5] W. Li, J. L. Yong, Q. Yang, F. Chen, Y. Fang and X. Hou, *Acta Phys. -Chem. Sin.*, 2018, **34**, 456-475.
- [6] https://en.wikipedia.org/wiki/Exxon_Valdez_oil_spill
- [7] https://en.wikipedia.org/wiki/Prestige_oil_spill
- [8] https://en.wikipedia.org/wiki/Deepwater_Horizon_oil_spill
- [9] http://www.cnn.com/2010/US/08/05/gulf.worst.disaster/index.html
- [10] C.-F. Wang, F.-S. Tzeng, H.-G. Chen and C.-J. Chang, *Langmuir*, 2012, **28**, 10015-10019.
- [11] J. L. Yong, F. Chen, Q. Yang, G. Du, C. Shan, J. Huo, Y. Fang and X. Hou, *Adv. Mater. Interfaces*, 2016, **3**, 1500650.
- [12] K. Li, J. Ju, Z. Xue, J. Ma, L. Feng, S. Gao and L. Jiang, *Nat. Commun.*, 2013, **4**, 2276.
- [13] L. Feng, Z. Zhang, Z. Mai, Y. Ma, B. Liu, L. Jiang and D. Zhu, *Angew. Chem. Int. Ed.*, 2004, **43**, 2012-2014.

- [14] S. Wang, Y. Song and L. Jiang, *Nanotechnology*, 2007, **18**, 015103. View Article Online DOI: 10.1039/C8CP04009E
- [15] L.-H. Kong, X.-H. Chen, L.-G. Yu, Z.-S. Wu and P.-Y. Zhang, *ACS Appl. Mater. Interfaces*, 2015, **7**, 2616-2625.
- [16] J. Song, S. Huang, Y. Lu, X. Bu, J. E. Mates, A. Ghosh, R. Ganguly, C. J. Carmalt, I. P. Parkin, W. Xu and C. M. Megaridis, *ACS Appl. Mater. Interfaces*, 2014, **6**, 19858-19865.
- [17] J. Li, R. Kang, X. Tang, H. She, Y. Yang and F. Zha, *Nanoscale*, 2016, **8**, 7638-7648.
- [18] J. Y. Huang, S. H. Li, M. Z. Ge, L. N. Wang, T. L. Xing, G. Q. Chen, X. F. Liu, S. S. Al-Deyab, K. Q. Zhang, T. Chen and Y. K. Lai, *J. Mater. Chem. A*, 2015, **3**, 2825-2832.
- [19] C.-H. Xue, Y.-R. Li, J.-L. Hou, L. Zheng, J.-Z. Ma, J. Mater. Chem. A, 2015, 3, 10248-10253.
- [20] J. L. Yong, Y. Fang, F. Chen, J. Huo, Q. Yang, H. Bian, G. Du and X. Hou, *Appl. Surf. Sci.*, 2016, **389**, 1148-1155.
- [21] Z. Xue, S. Wang, L. Lin, L. Chen, M. Liu, L. Feng and L. Jiang, *Adv. Mater.*, 2011, **23**, 4270-4273.
- [22] Q. Wen, J. Di, L. Jiang, J. Yu and R. Xu, Chem. Sci., 2013, 4, 591-595.
- [23] Y.-Q. Liu, Y.-L. Zhang, X.-Y. Fu and H.-B. Sun, *ACS Appl. Mater. Interfaces*, 2015, **7**, 20930-20936.
- [24] F. Zhang, W. B. Zhang, Z. Shi, D. Wang, J. Jin and L. Jiang, *Adv. Mater.*, 2013, **25**, 4192-4198.
- [25] E. Zhang, Z. Cheng, T. Lv, Y. Qian and Y. Liu, *J. Mater. Chem. A*, 2015, **3**, 13411-13417.
- [26] Z. Yu, F. Yun, Z. Gong, Q. Yao, S. Dou, K. Liu, L. Jiang and X. Wang, *J. Mater. Chem. A*, 2017, **5**, 10821-10826.
- [27] M. Tao, L. Xue, F. Liu and L. Jiang, Adv. Mater., 2014, 26, 2943-2948.
- [28] X. Gao, L.-P. Xu, Z. Xue, L. Feng, J. Peng, Y. Wen, S. Wang, X. Zhang, *Adv. Mater.*, 2014, **26**, 1771-1775.
- [29] G. Li, H. Fan, F. Ren, C. Zhou, Z. Zhang, B. Xu, S. Wu, Y. Hu, W. Zhu, J. Li, Y. Zeng, X. Li, J. Chu and D. Wu, *J. Mater. Chem. A*, 2016, **4**, 18832-18840.
- [30] Q. Zhu, Q. Pan and F. Liu, J. Phys. Chem. C, 2011, 115, 17464-17470.
- [31] Q. Zhu and Q. Pan, ACS Nano, 2014, 8, 1402-1409.
- [32] R. Du, X. Gao, Q. Feng, Q. Zhao, P. Li, S. Deng, L. Shi and J. Zhang, *Adv. Mater.*, 2016, **28**, 936-942.
- [33] C. Cao, M. Ge, J. Huang, S. Li, S. Deng, S. Zhang, Z. Chen, K. Zhang, S. S. Al-Deyab and Y. Lai, *J. Mater. Chem. A*, 2016, **4**, 12179-12187.
- [34] S.-J. Choi, T.-H. Kwon, H. Im, D.-I. Moon, D. J. Baek, M.-L. Seol, J. P. Duarte and Y.-K. Choi, *ACS Appl. Mater. Interfaces*, 2011, **3**, 4552-4556.
- [35] L. Su, H. Wang, M. Niu, X. Fan, M. Ma, Z. Shi and S.-W. Guo, *ACS Nano*, 2018, **12**, 3103-3111.
- [36] J. L. Yong, F. Chen, Q. Yang, J. Huo and X. Hou, *Chem. Soc. Rev.*, 2017, **46**, 4168-4217.
- [37] B. Su, Y. Tian and L. Jiang, J. Am. Chem. Soc., 2016, **138**, 1727-1748.

[38] Y. Tian, B. Su and L. Jiang, Adv. Mater., 2014, 26, 6872-6894.

View Article Online DOI: 10.1039/C8CP04009E

- [39] K. Liu, X. Yao and L. Lei, Chem. Soc. Rev., 2010, 39, 3240-3255.
- [40] L. Wen, Y. Tian and L. Lei, Angew. Chem. Int. Ed., 2015, 54, 3387-3399.
- [41] J. L. Yong, F. Chen, Q. Yang, Z. Jiang and X. Hou, *Adv. Mater.*, 2018, **5**, 1701370.
- [42] X. Yao, Y. Song and L. Jiang, Adv. Mater., 2011, 23, 719-734.

Published on 17 September 2018. Downloaded by Gazi Universitesi on 9/17/2018 5:30:59 AM

- [43] J. L. Yong, F. Chen, Q. Yang and X. Hou, Soft Matter, 2015, 11, 8897-8906.
- [44] J. L. Yong, F. Chen, M. Li, Q. Yang, Y. Fang, J. Huo and X. Hou, *J. Mater. Chem. A*, 2017, **5**, 25249-25257.
- [45] J. L. Yong, F. Chen, J. Huo, Y. Fang, Q. Yang, H. Bian, W. Li, Y. Wei and X. Hou, *ACS Omega*, **2018**, *3*, 1395-1402.
- [46] Y. Yu, H. Chen, Y. Liu, V. Craig, L. H. Li and Y. Chen, *Adv. Mater. Interfaces*, 2014, **1**, 1300002.
- [47] X. Zhou, Z. Zhang, X. Xu, F. Guo, X. Zhu, X. Men and B. Ge, *ACS Appl. Mater. Interfaces*, 2013, **5**, 7208-7214.
- [48] Y. Cao, X. Zhang, L. Tao, K. Li, Z. Xue, L. Feng and Y. Wei, *ACS Appl. Mater. Interfaces*, 2013, **5**, 4438-4442.
- [49] B. Cortese, D. Caschera, F. Federici, G. Ingo and G. Gigli, *J. Mater. Chem. A*, 2014, **2**, 6781-6789.
- [50] D. Tian, X. Zhang, X. Wang, J. Zhai and L. Jiang, *Phys. Chem. Chem. Phys.*, 2011, **13**, 14606-14610.
- [51] C. Wang, T. Yao, J. Wu, C. Ma, Z. Fan, Z. Wang, Y. Cheng, Q. Lin and B. Yang, *ACS Appl. Mater. Interfaces*, 2009, **11**, 2613-2617.
- [52] X. Zhang, Z. Li, k. Liu and L. Jiang, Adv. Funct. Mater., 2013, 23, 2881-2886.
- [53] X. Gao, J. Zhou, R. Du, Z. Xie, S. Deng, R. Liu, Z. Liu and J. Zhang, *Adv. Mater.*, 2016, **28**, 168-173.
- [54] Y. Liu, K. Zhang, W. Yao, C. Zhang, Z. Han and L. Ren, *Ind. Eng. Chem. Res.*, 2016, **55**, 2704-2712.
- [55] W. Zhou, S. Li, Y. Liu, Z. Xu, S. Wei, G. Wang, J. Lian and Q. Jiang, *ACS Appl. Mater. Interfaces*, 2018, **10**, 9841-9848.
- [56] F. Wang, S. Lei, M. Xue, J. Ou, C. Li and W. Li, *J. Phys. Chem. C*, 2014, **118**, 6344-6351.
- [57] F. Wang, S. Lei, M. Xue, J. Ou and W. Li, *Langmuir*, 2014, **30**, 1281-1289.
- [58] D. La, T. A. Nguyen, S. Lee, J. W. Kim and Y. S. Kim, *Appl. Surf. Sci.*, 2011, **257**, 5705-5710.
- [59] C. R. Crick, J. A. Gibbins and I. P. Parkin, *J. Mater. Chem. A*, 2013, **1**, 5943-5948.
- [60] A. K. Singh and J. K, Singh, RSC Adv., 2016, 6, 103632-103640.
- [61] M. Obaid, C. M. K. Tolba, M. Motlak, O. A. Fadali, K. A. Khalil, A. A. Almajid, B. Kim and N. A. M. Barakat, *Chem. Eng. J.*, 2015, **279**, 631-638.
- [62] S. O. Alayande, E. O. Dare, T. A. M. Msagati, A. K. Akinlabi and P. O. Aiyedun, *Phys. Chem. Earth*, 2016, **92**, 7-13.
- [63] W. Zhang, Y. Zhu, X. Liu, D. Wang, J. Li, L. Jiang and J. Jin, *Angew. Chem. Int. Ed.*, 2015, **53**, 856-860.

- [64] Y. Zhu, F. Zhang, D. Wang, X. Pei, W. Zhang and J. Jin, J. Mater. Chem. A^{View Article Online} 2013, 1, 5758-5765.
- [65] D. Tian, X. Zhang, Y. Tian, Y. Wu, X. Wang, J. Zhai and L. Jiang, *J. Mater. Chem.*, 2012, **22**, 19652-19657.
- [66 L. Li, Z. Liu, Q. Zhang, C. Meng, T. Zhang and J. Zhai, *J. Mater. Chem. A*, 2015, **3**, 1279-1286.
- [67] J. Li, L. Yan, H. Li, W. Li, F. Zha and Z. Lei, *J. Mater. Chem. A*, 2015, **3**, 14696-14702.
- [68] Z. Lian, J. Xu, Z. Wang, Z. Yu, Z. Weng and H. Yu, *Langmuir*, 2018, **34**, 2981-2988.
- [69] Q. Liu, A. A. Patel and L. Liu, ACS Appl. Mater. Interfaces, 2014, 6, 8996-9003.
- [70] K. He, H. Duan, G. Chen, H. Liu, W. Yang and D. Wang, *ACS Nano*, 2015, **9**, 9188-9198.
- [71] G. J. Dunderdale, C. Urata, T. Sato, M. W. England and A. Hozumi, *ACS Appl. Mater. Interfaces*, 2015, **34**, 18915-18919.
- [72] Y. Dong, J. Li, L. Shi, X. Wang, Z. Guo and W. Liu, *Chem. Commun.*, 2014, **50**, 5586-5589.
- [73] B. Wang and Z. Guo, Chem. Commun., 2013, 49, 9416-9418.
- [74] Z. Cheng, J. Wang, H. Lai, Y. Du, R. Hou, C. Li, N. Q. Zhang and K. N. Sun, *Langmuir*, 2015, **31**, 1393-1399.
- [75] R. Yang, P. Moni and K. K. Gleason, *Adv Mater Interfaces*, 2014, 1, 1400489.
- [76] M. A. Gondal, M. S. Sadullah, M. A. Dastageer, G. H. McKinley, D. Panchanathan and K. K. Varanasi, *ACS Appl. Mater. Interfaces*, 2014, **6**, 13422-13429.
- [77] M. Joo, J. Shin, J. Kim, J. B. You, Y. Yoo, M. J. Kwak, M. S. Oh and S. G. Im, *J. Am. Chem. Soc.*, 2017, **139**, 2329-2337.
- [78] J. P. Chaudhary, S. K. Nataraj, A. Gogda and R. Meena, *Green Chem.*, 2014, **16**, 4552-4558.
- [79] G. J. Dunderdale, M. W. England, T. Sato, C. Urata and A. Hozumi, *Macromol. Mater. Eng.*, 2016, **301**, 1032-1036.
- [80] G. Kwon, A. K. Kota, Y. Li, A. Sohani, J. M. Mabry and A. Tuteja, *Adv. Mater.*, 2012, **24**, 3666-3671.
- [81] R. Du, Z. Zheng, N. Mao, N. Zhang, W. Hu and J. Zhang, *Adv. Sci.*, 2015, **2**, 1400006.
- [82] P. Zhai, H. Jia, Z. Zheng, C. Lee, H. Su, T. Wei and S. Feng, *Adv. Mater. Interfaces*, 2015, **2**, 1500243.
- [83] Y. Gao, Y. S. Zhou, W. Xiong, M. Wang, L. Fan, H. Rabiee-Golgir, L. Jiang, W. Hou, X. Huang, L. Jiang, J-F. Silvain and Y. F. Lu, *ACS Appl. Mater. Interfaces*, 2014, **6**, 5924-5929.
- [84] J. Li, L. Yan, X. Tang, H. Feng, D. Hu and F. Zha, *Adv. Mater. Interfacs*, 2016, **3**, 1500770.
- [85] Y. Pan, K. Shi, C. Peng, W. Wang, Z. Liu and X. Ji, *ACS Appl. Mater. Interfaces*, 2014, **6**, 8651-8659.
- [86] S. Yu, H. Tan, J. Wang, X. Liu and K. Zhou, ACS Appl. Mater. Interfaces, 2015,

7, 6745-6753. View Article Online DOI: 10.1039/C8CP04009E

- [87] J. Li, C. Xu, Y. Zhang, R. Wang, F. Zha and H. She, *J. Mater. Chem. A*, 2016, **4**, 15546-15553.
- [88] Q. Zhu, Y. Chu, Z. Wang, N. Chen, L. Lin, F. Liu and Q. Pan, *J. Mater. Chem. A*, 2013, **1**, 5386-5393.
- [89] X. Zhang, W. Zhu and I. Parkin, RSC Adv., 2017, 7, 31.
- [90] F. Zou, L. Peng, W. Fu, J. Zhang and Z. Li, RSC Adv., 2015, 5, 76346-76351.
- [91] X. Zhou, Z. Zhang, X. Xu, X. Men and X. Zhu, *Ind. Eng. Chem. Res.*, 2013, **52**, 9411-9416.
- [92] D. N. H. Tran, S. Kabiri, T. R. Sim and D. Losic, *Environ. Sci.: Water Rse. Technol.*, 2015, **1**, 298-305.
- [93] G. Hayase, K. Kanamori, M. Fukuchi, H. Kaji and K. Nakanishi, *Angew. Chem. Int. Ed.*, 2013, **52**, 1986-1989.
- [94] P. Calcahnile, D. Fragouli, I. S. Bayer, G. C. Anyfantis, L. Martiradonna, P. D. Cozzoli, R. Cingolani and A. Athanassiou, *ACS Nano*, 2012, **6**, 5413-5419.
- [95] V. H. Pham and J. H. Dickerson, *ACS Appl. Mater. Interfaces*, 2014, **6**, 14181-14188.
- [96] K. Jayaramulu, K. K. R. Datta, C. Rösler, M. Petr, M. Otyepka, R. Zboril and R. A. Fisher, *Angew. Chem. Int. Ed.*, 2016, **55**, 1178-1182.
- [97] O. Arslan, Z. Aytac and T. Uyar, ACS Appl. Mater. Interfaces 2016, 8, 19747-19754.
- [98] J. T. Korhonen, M. Kettunen, R. H. A. Ras and O. Ikkala, *ACS Appl. Mater. Interfaces*, 2011, **3**, 1813-1816.
- [99] P. Mishra and K. Balasubramanian, RSC. Adv., 2014, 4, 53291-53296.
- [100] N. T. Cervin, C. Aulin, P. T. Larsson and L. Wågberg, *Cellulose*, 2012, 19, 401-410.
- [101] M. Guix, J. Orozco, M. Garc á, W. Gao, S. Sattayasamitsathit, A. Merkoci, A. Escarpa and J. Wang, *ACS Nano*, 2012, **6**, 4445-4451.
- [102] J. L. Yong, F. Chen, Q. Yang, D. Zhang, U. Farooq, G. Du and X. Hou, *J. Mater. Chem. A*, 2014, **2**, 8790-8795.
- [103] J. L. Yong, F. Chen, Q. Yang, G. Du, C. Shan, H. Bian, U. Farooq and X. Hou, *J. Mater. Chem. A*, 2015, **3**, 9379-9384.
- [104] J. L. Yong, F. Chen, Q. Yang, U. Farooq and X. Hou, *J. Mater. Chem. A*, 2015, **3**, 10703-10709.
- [105] J. Li, C. Xu, C. Guo, H. Tian, F. Zha and L. Guo, *J. Mater. Chem. A*, 2018, **6**, 223-230.
- [106] M. Blanco, E. Fischer and E. Cabane, Adv. Mater. Interfaces, 2017, 4, 1700584.
- [107] J. Li, C. Xu, Y. Zhang, X. Tang, W. Qi and Q. Wang, J. Colloid Interface Sci., 2018, **511**, 233-242.
- [108] J. Li, Z. Zhao, D. Li, X. Tang, H. Feng, W. Qi and Q. Wang, *Appl. Surf. Sci.*, 2017, **419**, 869-874.
- [109] J. Li, D. Li, Y. Yang, J. Li, F. Zha and Z. Lei, *Green Chem.*, 2016, **18**, 541-549.
- [110] Y.-H. Lo, C.-Y. Yang, H.-K. Chang, W.-C. Hung and P.-Y. Chen, *Sci. Rep.*, 2017, **7**, 1426.

[111] A. M. Rather, N. Jana, P. Hazarika and U. Manna, J. Mater. Chem. A, 2017, 5 / C8CP04009E 23339-23348.

[112] Y. L. Han, M. Li, Q. Yang, G. Huang, H. Liu, Y. Qin, G. M. Genin, F. Li, T. J. Lu and F. Xu, *Adv. Funct. Mater.*, 2017, **27**, 1606607.

[113] Q. Meng, Q. Wang, H. Liu and L. Jiang, NPG Asia Mater., 2014, 6, e125.

A table of contents entry



This review summarizes the recent developments of oil/water separation by natural superwetting materials, including the superwettability, separating method, and mechanism.

Photograph and biography of authors



Dr. Jiale Yong is currently a lecturer of Electronic Science and Technology at Xi'an Jiaotong University. He received his BS degree from Xi'an Jiaotong University in 2011. After that, he joined Prof. Chen's research group and received a Ph.D. in Electronic Science and Technology from Xi'an Jiaotong University in 2016. His research interests include femtosecond laser microfabrication, controlling wettability of solid surfaces, and bioinspired designing superhydrophobic and superoleophobic interfaces.

View Article Online DOI: 10.1039/C8CP04009E



Dr. Jinglan Huo is currently a Ph.D. candidate in Prof. Feng Chen's research group at Xi'an Jiaotong University. She received her BS degree in Electronic and Information Engineering from Xidian University in 2015. Her research interests include femtosecond laser microfabrication, super-wettability, and cell engineering on superhydrophobic patterned microstructures.



Published on 17 September 2018. Downloaded by Gazi Universitesi on 9/17/2018 5:30:59 AM

Prof. Feng Chen is a full professor at the School of Electronics and Information Engineering at Xi'an Jiaotong University, where he directs the Femtosecond Laser Laboratory. He received a BS degree in physics from Sichuan University, China, in 1991, and then began to work for the Chinese Academy of Science (1991 to 2002), where he was promoted to a full professor in 1999. He received a Ph.D. in Optics from the Chinese Academy of Science in 1997. In 2002, he joined Xi'an Jiaotong University, where he became a group leader. His current research interests are femtosecond laser microfabrication and bionic microfabrication.

View Article Online DOI: 10.1039/C8CP04009E



Prof. Qing Yang received her BS degree in Photoelectron Science and Technology in 1992 from Sichuan University. In 2009, she received her Ph.D. from Xi'an Institute of Optics and Fine Mechanics, Chinese Academy of Science. She is currently an associate professor at Xi'an Jiaotong University. Her current research interests are femtosecond laser fine process, microfluidic biochips, and micro-photonics.



Prof. Xun Hou received his BS degree in Physics from Northwest University, China, in 1959. From Oct. 1979 to Nov. 1981, he worked at Imperial College in England as a visiting scholar. He was elected as an academician of Chinese Academy of Sciences in 1991. He currently is a professor of Xi'an Jiaotong University, and he is also the director of the Shaanxi Key Laboratory of Photonics Technology for Information. His research interests mainly focus on photoelectronic materials and devices.